zyg-11 and *cul-2* regulate progression through meiosis II and polarity establishment in *C. elegans*

Rémi Sonneville and Pierre Gönczy*

ISREC (Swiss Institute for Experimental Cancer Research), 155, chemin des Boveresses, CH-1066 Epalinges/Lausanne, Switzerland

*Author for correspondence (e-mail: pierre.gonczy@isrec.unil.ch)

Accepted 30 April 2004

Development 131, 3527-3543
Published by The Company of Biologists 2004
doi:10.1242/dev.01244

Summary

The mechanisms that ensure coupling between meiotic cell cycle progression and subsequent developmental events, including specification of embryonic axes, are poorly understood. Here, we establish that *zyg-11* and the cullin *cul-2* promote the metaphase-to-anaphase transition and M phase exit at meiosis II in *Caenorhabditis elegans*. Our results indicate that ZYG-11 acts with a CUL-2-based E3 ligase that is essential at meiosis II and that functions redundantly with the anaphase-promoting complex/cyclosome at meiosis I. Our data also indicate that delayed M phase exit in *zyg-11*(*RNAi*) embryos is due to accumulation of the B type cyclin CYB-3. We demonstrate that PAR proteins and P granules become polarized in an inverted manner during the meiosis II delay resulting from *zyg-11* or *cul-2* inactivation, and that *zyg-11* and *cul-2* can regulate polarity establishment independently of a role in cell cycle progression. Furthermore, we find that microtubules appear dispensable for ectopic polarity during the meiosis II delay in *zyg-11*(*RNAi*) embryos, as well as for AP polarity during the first mitotic cell cycle in wild-type embryos. Our findings suggest a model in which a CUL-2-based E3 ligase promotes cell cycle progression and prevents polarity establishment during meiosis II, and in which the centrosome acts as a cue to polarize the embryo along the AP axis after exit from the meiotic cell cycle.

Movies and supplemental data available online

Key words: Meiotic cell cycle, AP polarity, E3 ligase, *C. elegans*, APC

Introduction

The meiotic cell cycle differs from the mitotic cell cycle in several respects. One key difference lies in the fact that the two meiotic divisions occur without an intervening S phase, thus ensuring the generation of haploid gametes. Another distinctive feature is that exit from the meiotic cell cycle is followed by important developmental events such as embryonic axis specification. The mechanisms allowing progression through the meiotic cell cycle and their coupling to subsequent development are incompletely understood.

Progression through mitosis is governed by cyclin-dependent kinases (Cdks), which drive cells into metaphase, and by the anaphase-promoting complex/cyclosome (APC), a multi-subunit E3 ligase that poly-ubiquitinates substrate proteins to target them for destruction by the proteasome (reviewed by Nurse, 2002; Peters, 2002). APC substrates include securins, whose destruction is essential for the metaphase to anaphase transition, and B-type cyclins, whose destruction is essential for mitotic exit. Although the APC is a universal regulator of mitosis, the situation appears to be different during meiosis. In *Xenopus laevis*, the APC is required for the metaphase to anaphase transition of meiosis II, but not for that of meiosis I (Peter et al., 2001; Taieb et al., 2001). Conversely, in *C. elegans*, the APC is required at meiosis I but seemingly not at meiosis II (Golden et al., 2000; Shakes et al., 2003; Wallenfang and Seydoux, 2000). It is likely that components other than the APC ensure progression through meiosis I in *X. laevis* and meiosis II in *C. elegans*, although their identity is not known.

Progression through the mitotic cell cycle also requires cullin-based E3 ligases, including Skp1-Cul1-F-box-protein complexes (SCF) and Elongin C-Cul2-SOCS box complexes (ECS) (reviewed by Deshaies, 1999). In *Saccharomyces cerevisiae*, SCF activity is required at the G1 to S transition to target Cdk inhibitors for degradation (Schwob et al., 1994), and plays a role at the G2 to M transition as well (Goh and Surana, 1999). ECS activity is thought to be required for the G1 to S transition, as germ cells homozygous for a *cul-2* deletion in *C. elegans* accumulate in G1 (Feng et al., 1999). Although embryos lacking *cul-2* function often fail to extrude a second polar body (Feng et al., 1999), the exact requirement of cullin-based E3 ligases in meiotic cell cycle progression remains to be elucidated.

Establishment of polarity along the anteroposterior (AP) embryonic axis in *C. elegans* occurs shortly after exit from the meiotic cell cycle. The two female meiotic divisions take place shortly after fertilization, which occurs when the oocyte enters the spermatheca (McCarter et al., 1999). Because the nucleus is located distally in the mature oocyte, oocyte-derived chromosomes and the meiosis I and II spindles are on the distal side of the newly fertilized embryo, whereas sperm-derived chromosomes and centrosomes are on the proximal side. AP polarity is initiated by a sperm component that confers

posterior character to the proximal side and becomes apparent during S phase of the first mitotic cell cycle (Cuenca, 2003; Goldstein and Hird, 1996). This results in a polarized distribution of maternally contributed PAR and MEX proteins in the one-cell stage embryo (reviewed by Lyczak et al., 2002; Pellettieri and Seydoux, 2002; Rose and Kemphues, 1998). PAR-3 and PAR-6 localize to the anterior cortex, PAR-2 and PAR-1 localize to the posterior cortex, whereas MEX-5 and MEX-6 are restricted to the anterior cytoplasm. Polarity established by PAR and MEX proteins translates into differential segregation of developmental factors. For instance, P granules and PIE-1, which are both destined to the germ lineage, are segregated to the posterior of the one-cell stage embryo. Polarity also translates into asymmetric elongation of the mitotic spindle, resulting in an unequal first division that generates a larger anterior blastomere and a smaller posterior one.

The prevailing view is that the sperm component acting as polarity cue corresponds to astral microtubules nucleated by paternally contributed centrosomes. Relevant to this view are experiments conducted with conditional mutants in APC components. At the restrictive temperature, such mutants arrest at the metaphase to anaphase transition of meiosis I (Golden et al., 2000; Wallenfang and Seydoux, 2000). Approximately 40% of these embryos establish inverted polarity, with the posterior markers PAR-1, PAR-2 and PIE-1 enriched in the vicinity of the persisting meiotic spindle, and the anterior marker PAR-3 enriched on the opposite side (Wallenfang and Seydoux, 2000). The fraction of embryos with inverted polarity is halved when microtubules are depolymerized with nocodazole, and PIE-1 is no longer segregated when the meiotic spindle is lacking following inactivation of the *Cdc2* homologue *ncc-1* (Wallenfang and Seydoux, 2000). These observations suggest that microtubules from the persisting meiosis I spindle can act as a surrogate cue sufficient for polarity establishment. It has also been proposed that astral microtubules may be necessary, because polarity is not established in embryos with aberrant sperm asters that nucleate few astral microtubules following the inactivation of *air-1*, *spd-2* or *spd-5* (Hamill et al., 2002; O'Connell et al., 2000; Schumacher et al., 1998; Wallenfang and Seydoux, 2000). The APC itself has also been implicated in polarity establishment. Hypomorphic APC mutants that allow meiotic cell cycle completion result in polarity defects, which are also observed following mild inactivation of separase (Rappleye et al., 2002). However, the view that the APC plays a direct role in polarity establishment is controversial, because there is a strict correlation between defects in meiotic cell cycle progression and defects in polarity, suggesting that the latter may be a consequence of the former (Shakes et al., 2003).

zyg-11 is another component that appears to play a role in meiotic cell cycle progression and AP polarity. Analysis of live embryos from the temperature-sensitive allele *zyg-11*(*b2*), and of fixed specimens from the non-conditional allele *zyg-11*(*mn40*), indicate that *zyg-11* is required for progression through meiosis II (Kemphues et al., 1986). The division of *zyg-11(mn40)* one-cell stage embryos can be asymmetric as in wild type, yielding a larger anterior blastomere and a smaller posterior one, asymmetric but inverted, or symmetric (Kemphues et al., 1986). Moreover, P granules are mislocalized in *zyg-11*(*mn40*) embryos, further indicating that *zyg-11* is somehow required for proper AP polarity (Kemphues et al., 1986). Although defects are observed at later stages of embryogenesis, they probably reflect an earlier requirement for *zyg-11* function, as the temperature-sensitive period of *zyg-11*(*b2*) spans the time from fertilization until the end of meiosis II (Kemphues et al., 1986). *zyg-11* encodes a 799 amino acid protein that bears at least two leucine-rich repeats and one Armadillo repeat (Carter et al., 1990). There are ZYG-11 homologues in other metazoans, including *Drosophila* and human, suggesting that this family of proteins performs an evolutionarily conserved function.

Here, we establish that embryos with impaired *zyg-11* function have a delayed metaphase to anaphase transition and M phase exit at meiosis II. We find an identical phenotype after inactivating *cul-2* and suggest that ZYG-11 acts with a CUL-2-based E3 ligase during meiosis. We provide evidence that the B-type cyclin CYB-3 is a target of this E3 ligase at meiosis II. We uncover that PAR proteins and P granules become localized in an inverted manner during the meiosis II delay following *zyg-11* or *cul-2* inactivation, and establish that these two components can regulate polarity establishment independently of their role in cell cycle progression. Unexpectedly, we find that microtubules appear dispensable for ectopic polarity in embryos lacking *zyg-11* function, as well as for polarity establishment in wild-type embryos. We propose a model in which the centrosome acts as a cue to polarize the embryo along the AP axis following exit from the meiotic cell cycle.

Materials and methods

Nematodes

C. elegans strains of the following genotypes were maintained according to standard procedures (Brenner, 1974): *him-1*(*e879*) I; *mnC1 dpy-10*(*e128*) *unc-52*(*e444*)/*zyg-11*(*mn40*) *unc-4*(*e120*) II (Kemphues et al., 1986); *cul-2*(*ek1*)/*unc-64*(*e246*) III (Feng et al., 1999), as well as *unc-32*(*e189*) *cul-2*(*t1644)* and *unc-32*(*e189*) *cul-2*(*t1664)*, both balanced by *qC1 dpy-19*(*e1259ts*) *glp-1*(*q339*) (Gönczy et al., 1999); *mat-1*(*ax161*) I; *him-8*(*e1489*) IV and *mat-1*(*ax144*) I; *him-8*(*e1489*) IV (raised at 16°C and shifted 8-10 hours to 25°C for restrictive conditions) (Wallenfang and Seydoux, 2000); *nDf29*/*unc-13*(*e1091*) *spd-2*(*oj29*) I (O'Connell et al., 2000). Transgenic animals expressing GFP-histone2B (GFP-HIS), GFP-β-tubulin (GFP-TUB), GFP-PAR-2 and GFP-ZIF-1 have been described (DeRenzo et al., 2003; Strome et al., 2001; Wallenfang and Seydoux, 2000).

For generation of GFP-ZYG-11 and GFP-CYB-3 transgenic animals, PCR-derived genomic fragments (sequences of these and other primer pairs available upon request) were subcloned into pSU25, a modified version of the *pie-1-gfp* vector containing the *unc-119* cDNA (a gift from Michael Glotzer). Sequence-verified constructs were bombarded essentially as described (Praitis et al., 2001). For GFP-ZYG-11, two integrated and one non-integrated lines were retained. For GFP-CYB-3, one non-integrated line was recovered; GFP-CYB-3 was present within nuclei of oocytes and embryonic blastomeres throughout the cell cycle, and was released in the cytoplasm at NEBD (data not shown).

zyg-11 and *cul-2* mutant alleles

Most of the *zyg-11* coding sequence was sequenced following PCR reactions; a C to T alteration at position 483 of the *zyg-11* gene was found in *zyg-11*(*mn40*) in two independent PCR reactions, predicted to truncate ZYG-11 after amino acid 161.

Two alleles (*t1664* and *t1644*) of a maternal-effect locus mapping close to *cul-2* give rise to a phenotype similar to that of *cul-2*(*RNAi*)

(Gönczy et al., 1999). Sequencing of RT-PCR products and parts of the *cul-2* genomic sequence following PCR reactions revealed mutations in the donor site of the third intron (G to A alteration at position 1200 of the gene in *t1664*) or the fourth intron (G to A alteration at position 1472 of the gene in *t1644*). Both mutations result in the use of a new donor site (G at position 1152 for *t1664*, G at position 1496 for *t1644*) predicted to yield a protein truncation and an internal deletion, respectively.

RNAi

RNAi feeding strains for *zyg-11*, *cul-2* (a gift from Lionel Pintard), *cyb-3*, *elc-1*, *ncc-1* and *tba-2* (a gift from Michael Glotzer) were generated essentially as described (Timmons et al., 2001). The *mat-1* feeding strain was from the chromosome I feeding library (Fraser et al., 2000). RNAi was performed by feeding L4 larvae for 24-36 hours essentially as described (Kamath et al., 2001).

Slightly milder conditions were used for *zyg-11*(*RNAi*) embryos expressing GFP-HIS, GFP-TUB and GFP-PAR-2 to improve recovery. Although this reduced the frequency of chromosome segregation defects, inverted polarity was nevertheless always established during the meiosis II delay under these conditions (see Fig. 7). Of 25 embryos analyzed in this manner, 6 failed to develop until the two-cell stage and were not considered for analysis.

The penetrance of the *tba-2*(*RNAi*) phenotype was somewhat variable. Those embryos with microtubule remnants were not retained for analysis; occasional gigantic polyploid embryos, which probably resulted from oocyte fusion events, were also not retained. Most reliable phenotypes were obtained after feeding for 28 hours for wild-type and 34 hours for *zyg-11*(*mn40*). Shorter feeding resulted in more embryos with partial inactivation, longer feeding in more gigantic embryos. In the absence of a first polar body, *zyg-11*(*mn40*) *tba-2*(*RNAi*) embryos at meiosis II were distinguished from those at meiosis I by the fact that the former are slightly smaller, being separated from the eggshell, and have a more intact cortex after fixation and staining than meiosis I embryos.

The following 26 genes were inactivated using RNAi by feeding to search for components required for meiosis II. Ten were genes whose reported phenotype was potentially similar to that of *zyg-11*(*RNAi*), C47B2.4 (*pbs-2*), F25H2.9 (*pas-5*), F33D11.10, F39H11.5 (*pbs-7*), F48E8.5 (*paa-1*), K07C11.2 (*air-1*), T09A5.9, Y45F10A.2 (*puf-3*), ZK1127.5, ZK520.4 (*cul-2*); 10 were putative cell cycle regulators, C09G4.3 (*cks-1*), H31G24.4 (*cyb-2.2*), K06A5.7a (*cdc-25.1*), T05A6.1 (*cki-1*), T05A6.2a (*cki-2*), T06E6.2 (*cyb-3*), W02A2.6 (*rec-8*), Y60A3A.12 (*chk-2*), ZC168.4 (*cyb-1*), ZK1307.6 (*fzr-1*); and six were genes with homologies to *zyg-11*, C33A12.12, Y9C9A.13, Y39G10AR.5, F44E5.2, F47D12.5, T24C4.6.

Microscopy

Pressure-free and isotonic conditions (Shelton and Bowerman, 1996) were used because embryos shortly after fertilization are fragile. To achieve precise timing of events, embryos were imaged essentially as described (Brauchle et al., 2003), collecting 1 frame every 30 seconds either in utero, starting at fertilization, or ex utero, starting before anaphase I. Duration of events obtained with either method was comparable. For in utero recordings, 4-10 worms were soaked for ~45 minutes in M9 buffer, supplemented with 0.01% tetramisole and 0.1% Tricaine (Kirby et al., 1990), and mounted under a cover-slip on a 2% agarose pad surrounded by vaseline. For visualizing chromosomes in live embryos expressing GFP-PAR-2 and that are osmosensitive, samples were bathed in Hoechst 33342 for four minutes and then washed for two minutes prior to imaging.

Fixation and indirect immunofluorescence were essentially as described (Gönczy et al., 1999). Primary antibodies were mouse anti-tubulin (DM1A; 1:400; Sigma) and the following antibodies raised in rabbits: anti-PAR-1 (1:2000) (Gönczy et al., 2001), anti-PAR-2 (1:400) (Pichler et al., 2000), anti-PAR-3 (1:60) (Pichler et al., 2000), anti-PGL-1 (1:2000) (Kawasaki et al., 1998), anti-SAS-4 (1:1600) (Leidel and Gönczy, 2003), anti-phosphorylated histone H3 (1:1200; Upstate) and anti-GFP (1:600, a gift from Viesturs Simanis). Slides were counterstained with Hoechst 33258 (Sigma) to reveal DNA. Indirect immunofluorescence was imaged on an LSM510 Zeiss confocal microscope; quantification of GFP-CYB-3, GFP-ZYG-11 and GFP-ZIF-1 signals was performed using a 12-bit CCD Camera and Metamorph software (Universal Imaging). Images were processed with Adobe Photoshop.

Results

zyg-11 is required for timely metaphase to anaphase transition and M phase exit at meiosis II

To analyze the consequences of *zyg-11* inactivation with high temporal and spatial resolution, we performed dual differential interference contrast (DIC) and fluorescence time-lapse microscopy using transgenic animals expressing GFP-HIS (histone 2B). In wild type (Fig. 1, Fig. 2A-C, Table 1; see Table S1 and Movies 1 and 2 at http://dev.biologists.org/supplemental/), the meiosis I spindle assembles shortly after fertilization. Following the metaphase to anaphase transition of meiosis I, homologous chromosomes segregate during anaphase I and extrusion of the first polar body ensues. After a brief time interval that we refer to as meiotic interphase, the meiosis II spindle assembles. Following the metaphase to anaphase transition of meiosis II, sister chromatids segregate during anaphase II, after which the second polar body is extruded. Embryos then exit the meiotic cell cycle, oocyte- and sperm-derived chromosomes decondense as pronuclei form and the first mitotic cell cycle ensues.

We analyzed *zyg-11*(*RNAi*) embryos and *zyg-11*(*mn40*) mutant embryos, which are likely to be null for *zyg-11* function (see Materials and methods). In both cases (Fig. 1, Fig. 2G-J, Table 1; Table S1 and Movie 3 at http://dev.biologists.org/supplemental/), the timing of events is indistinguishable from wild type prior to the metaphase of meiosis II. However, the metaphase to anaphase transition of meiosis II is significantly delayed, with embryos exhibiting metaphase-like figures for ~30 minutes, as compared with ~6 minutes in wild type. During this delay, chromosomes lose their tight arrangement on the metaphase plate and the spindle becomes less organized (Fig. 2I). Thereafter, anaphase-like figures are observed, although chromosome bridges are often apparent and sister chromatids are not segregated properly (Fig. 2J). Moreover, anaphase II is lengthened. Chromosomes display the M phase-specific phosphorylated histone H3 (Hsu et al., 2000) throughout the meiosis II delay in *zyg-11*(*RNAi*) embryos, including when anaphase-like configurations are apparent, indicating that it corresponds to a prolonged M phase (Fig. 2L-N). Eventually, oocyte and sperm-derived chromosomes decondense, pronuclei form and the first mitotic cell cycle ensues. We conclude that *zyg-11* is required for timely metaphase to anaphase transition and M phase exit at meiosis II.

cyb-3 and *cul-2* are also required for meiosis II progression

As the sequence of ZYG-11 does not offer obvious clues as to its biochemical activity, we sought to identify other genes whose inactivation results in delayed progression through meiosis II to gain insight into the mechanism of action of

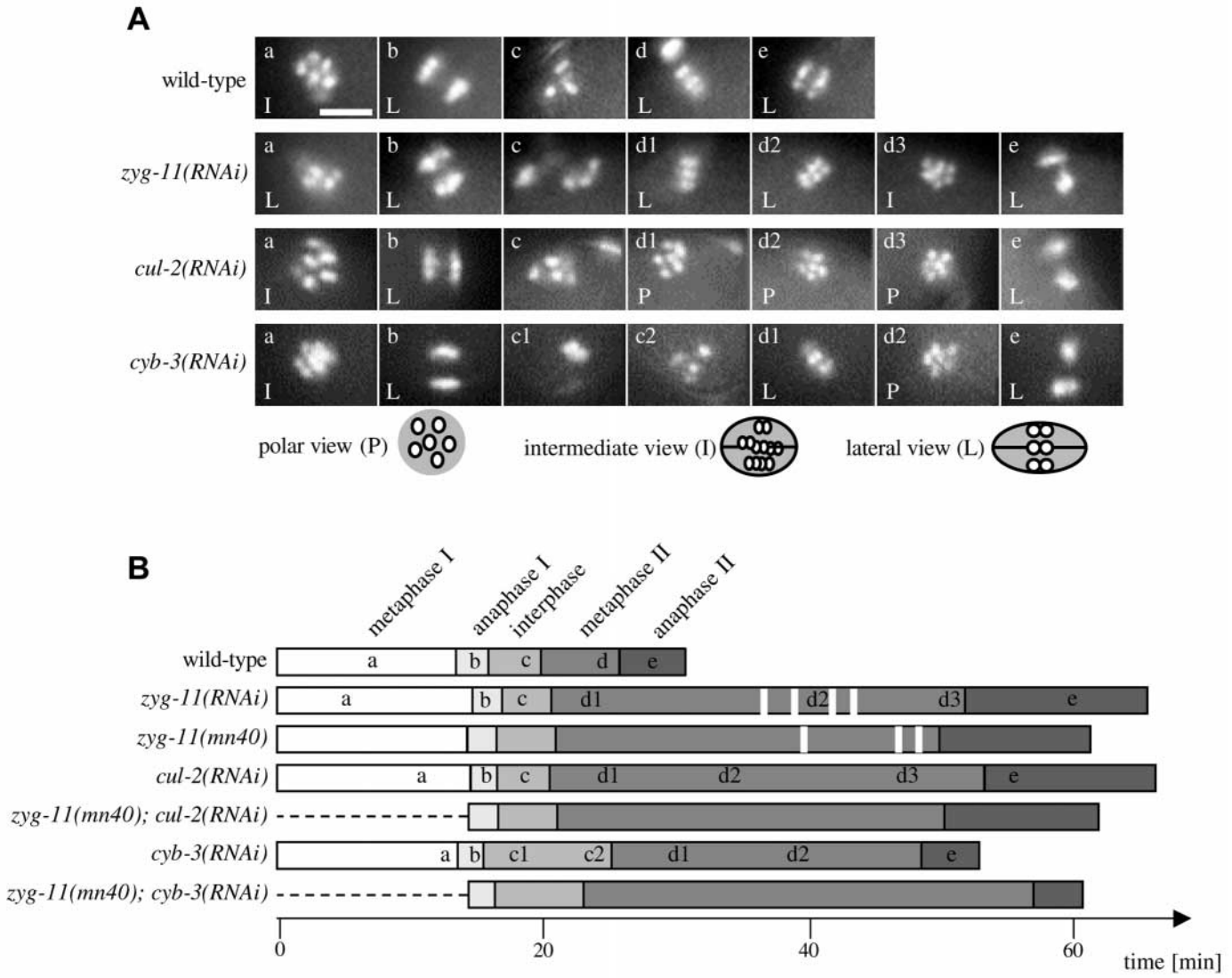

Fig. 1. *zyg-11*, *cul-2* and *cyb-3* are required for progression through meiosis II. (A) Images from time-lapse sequences of embryos expressing GFP-HIS (see also Movies 1-7 at http://dev.biologists.org/supplemental/). Metaphase views are: polar (P), the spindle is viewed from the pole and five homologues (meiosis I) or sister chromatids (meiosis II) are observed in a circle around the sixth; lateral (L), the spindle is viewed from the side and up to three pairs of homologues (meiosis I) or sister chromatids (meiosis II) are observed; or intermediate (I), between the polar and lateral views. In this and other figures, embryos are oriented with polar bodies to the left and all panels of a kind are at the same magnification. Scale bar: 5 μm. (B) Timing of events in embryos from fertilization (t=0) until the end of meiosis II. Average duration of each stage, defined in Table 1, is indicated. Letters in the time-lines indicate the time at which the corresponding images in (A) are taken. Vertical white lines indicate the time at which GFP-PAR-2 first becomes enriched at the cell cortex in the vicinity of oocyte-derived chromosomes in *zyg-11*(*RNAi*) (*n*=4) or *zyg-11*(*mn40*) (*n*=3) embryos imaged starting at the end of meiosis I.

ZYG-11. We examined the results of RNAi-based functional genomic screens available as DIC movies through www.wormbase.org. Out of ~5500 genes considered, we found 10 whose reported phenotype resembles that of *zyg-11*(*RNAi*). We also selected 10 putative cell cycle regulators and six ORFs that bear homology with *zyg-11* for further analysis (see list of genes in Materials and methods). We inactivated these 26 genes using RNAi and analyzed meiotic cell cycle progression using time-lapse DIC microscopy. We found two genes whose inactivation does not affect meiosis I but results in delayed progression through metaphase of meiosis II: the B type cyclin *cyb-3* and the cullin *cul-2*.

In *cyb-3*(*RNAi*) embryos (Fig. 1, Table 1; Table S1 and Movie 4 at http://dev.biologists.org/supplemental/), the delay is already apparent prior to metaphase, earlier than in the absence of *zyg-11* function. Another difference is that anaphase II is not delayed in *cyb-3*(*RNAi*) embryos. By contrast, we found that *cul-2*(*RNAi*) embryos (Fig. 1, Table 1; Table S1 and Movie 5 at http://dev.biologists.org/supplemental/) have a meiotic phenotype indistinguishable from that of *zyg-11*(*RNAi*) or *zyg-11*(*mn40*) embryos. In particular, the metaphase to anaphase transition of meiosis II is significantly delayed, with embryos exhibiting metaphase-like figures for ~33 minutes. Moreover, anaphase II is lengthened and often aberrant. We

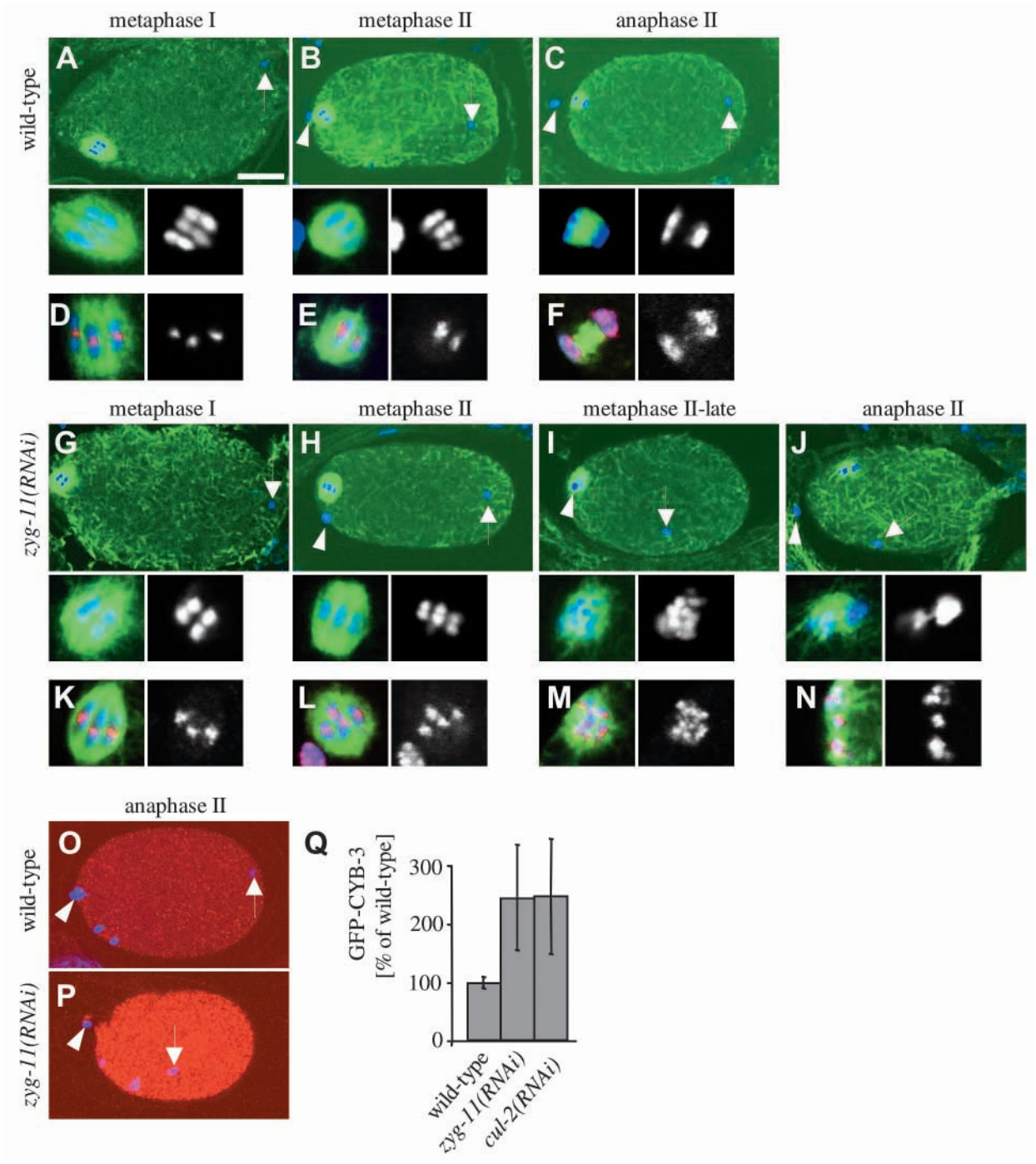

Fig. 2. *zyg-11* is required for timely metaphase to anaphase transition and M phase exit at meiosis II. (A-N) Lateral views of wild-type or *zyg-11*(*RNAi*) embryos at the indicated stages, stained with antibodies against α-tubulin (A-C,G-J), or α-tubulin and phosphorylated histone H3 (D-F,K-N). Insets below panels A-C and G-J, as well as the entire panels D-F and K-N are magnified views of a meiotic spindle and have a width of ~7 μm. Insets below panels A-C and G-J show α-tubulin (green) and DNA (blue) on the left, and DNA alone on the right. Panels D-F and K-N show α-tubulin (green), phosphorylated histone H3 (red) and DNA (blue) on the left, and phosphorylated histone H3 alone on the right. To view polar bodies and sperm chromosomes, the DNA signal in the low magnification images is a projection of several 1-μm confocal optical sections. Arrowheads point to the first polar body, arrows indicate condensed sperm DNA. Scale bar: 10 μm. Note that the focus of phosphorylated H3 lies between homologues at metaphase I and sister chromatids at metaphase II in both wild-type and *zyg-11*(*RNAi*) embryos. (O,P) Wild-type (O) and *zyg-11*(*RNAi*) (P) anaphase II embryos expressing GFP-CYB-3 stained with antibodies against α-tubulin (not shown) and GFP (red); DNA is shown in blue. (Q) Quantification of signal intensities in wild-type (n=6), *zyg-11*(*RNAi*) (n=14) and *cul-2*(*RNAi*) (n=19) embryos in metaphase II or anaphase II stained as in (O); embryos were staged using the anti-α-tubulin and DNA signals. The difference between wild type and *zyg-11*(*RNAi*) or *cul-2*(*RNAi*) is statistically significant (Student's t-test: $P=6\times10^{-5}$ and $P=4\times10^{-6}$, respectively).

Table 1. Duration of events during meiosis in wild type, and following *zyg-11*, *cul-2* or *cyb-3* inactivation

	Metaphase I	Anaphase I	Interphase	Metaphase II	Anaphase II
Wild type	13′39″+/-1′24″	2′26″+/-0′36″	4′01″±0′54″	6′03″±0′37″	5′04″±0′55″
n=	10	10	10	10	10
zyg-11(RNAi)	14′51″±2′38″	2′18″±0′44″	3′40″±0′52″	31′25″±3′05″	13′54″±7′11″
n=	11	12	12	10	11
zyg-11(mn40)	14′34″±1′31″	2′15″±0′44″	4′30″±1′25″	29′18″±10′40″	11′31″±6′55″
n=	9	11	11	13	10
cul-2(RNAi)	14′43″±2′38″	1′58″±0′40″	4′05″±0′39″	33′11″ ±7′01″	12′58″±6′56″
n=	12	17	17	13	10
cyb-3(RNAi)	13′46″±0′54″	2′00″±0′05″	9′41″±2′09″	23′36″±4′03″	4′20″±0′56″
n=	6	5	5	8	7
zyg-11(mn40); cul-2(RNAi)	ND	2′13″±0′33″	4′25″±1′07″	29′28″±7′45″	11′48″±4′13″
n=		9	9	9	9
zyg-11(mn40); cyb-3(RNAi)	15′04″	2′03″±0′23″	6′46″±2′07″	34′16″±7′28″	3′49″±1′36″
n=	1	7	7	8	11

Average duration of meiotic events in minutes and seconds, along with standard deviation, in embryos of the indicated genotypes as determined by dual DIC and fluorescent time-lapse recordings of animals expressing GFP-HIS (some wild-type and *zyg-11*(*RNAi*) embryos carried GFP-TUB in addition). n, number of embryos scored for each stage. ND, not determined.

Stages were defined as follows. Metaphase I: from when the oocyte enters the spermatheca (fertilization) until the onset of homologous chromosome segregation. Anaphase I: from the end of metaphase I stage until extrusion of first polar body. Interphase: from the end of anaphase I stage until sister chromatids are aligned on the metaphase plate of meiosis II. Metaphase II: from the end of interphase stage until the onset of sister chromatid segregation. Anaphase II: from the end of metaphase II stage until the first pronucleus become visible and chromosomes decondense, chosen as an end-point because the polar body is often not extruded in delayed embryos. The duration of bona fide anaphase+telophase II in the wild type is 1′59″±0′19″. One series of *zyg-11*(*mn40*) *cul-2*(*RNAi*) embryos (out of four experiments) is not shown here as all embryos were extremely delayed, probably due to excess photodamage.

cul-2(*ek1*) embryos were timed in utero by time-lapse DIC microscopy, scoring extrusion of the first polar body and pronuclear formation as landmarks, with the following outcome: meiosis I (metI+anaI), 20′02″±1′11″ (*n*=10); meiosis II (inter+metII+anaII), 46′51″±8′19′ (*n*=9). Meiosis I appears to be slightly longer than in *cul-2*(*RNAi*) (where it is 16′41″), probably because of the inherent imprecision in timing polar body extrusion in utero.

found a similar phenotype in the deletion allele *cul-2*(*ek1*), and in two maternal-effect embryonic lethal alleles of *cul-2* (Table 1; see Materials and methods). Importantly, inactivation of *cul-2* by RNAi in *zyg-11*(*mn40*) mutant embryos does not result in a more prolonged meiosis II delay (Fig. 1, Table 1; see Movie 6 at http://dev.biologists.org/supplemental/), compatible with the notion that *zyg-11* and *cul-2* act in a common process. A phenotype similar to that observed by inactivating *zyg-11* or *cul-2* has also been obtained by inactivating Elongin C (*elc-1*) and Rbx (*rbx-1*), two other core components of ECS E3 ligases (Liu et al., 2004). Taken together, these results establish that a CUL-2-containing E3 ligase is essential for timely metaphase to anaphase transition and M phase exit at meiosis II, and suggest that ZYG-11 somehow acts in concert with this ECS.

CYB-3 accumulates following *zyg-11* inactivation, delaying M phase exit

Given that *cyb-3* acts at meiosis II, and that degradation of B type cyclins is generally required for M phase exit, we investigated whether persistence of CYB-3 may be causing delayed M phase exit when the CUL-2-based E3 ligase is inactivated. We generated a fusion protein between GFP and CYB-3; in wild type, we found levels of GFP-CYB-3 to be high until metaphase I, and significantly lower after the metaphase to anaphase transition of meiosis I (data not shown). Similar low levels were observed during meiosis II (Fig. 2O), although these low levels precluded assessing whether levels drop further after the metaphase to anaphase transition of meiosis II. Importantly, we found that GFP-CYB-3 levels during the meoisis II delay in *zyg-11*(*RNAi*) and *cul-2*(*RNAi*) embryos were high compared with wild-type meiosis II embryos (Fig. 2P,Q). To test whether CYB-3 accumulation was causing delayed M phase exit in the absence of *zyg-11* function, we examined *zyg-11*(*mn40*) *cyb-3*(*RNAi*) embryos. Strikingly, whereas the metaphase to anaphase transition of meiosis II is still delayed in such embryos, the anaphase II delay is abolished (Fig. 1, Table 1; see Movie 7 at http://dev.biologists.org/supplemental/). Therefore, the persistence of CYB-3 appears to be responsible for delayed M phase exit following *zyg-11* inactivation.

ZYG-11 may be a substrate recruitment subunit of a meiosis-specific CUL-2-containing ECS

ECS E3 ligases contain a SOCS-box-containing protein that bridges Elongin C and the substrate (Kile et al., 2002). We considered whether ZYG-11 could be such a substrate recruitment subunit, even though it does not contain an obvious SOCS-box. Substrate recruitment subunits of the ECS and other cullin-based E3 ligases are unstable and are targeted for degradation by the very same complex of which they are a part (DeRenzo et al., 2003; Galan and Peter, 1999; Geyer et al., 2003; Pintard et al., 2003b; Wirbelauer et al., 2000; Zhou and Howley, 1998). To test whether ZYG-11 behaves in this manner, we generated a transgenic line expressing GFP-ZYG-11 and compared GFP levels in wild-type and *cul-2*(*RNAi*) animals. Although wild-type animals express the fusion protein at very low levels in the germ-line and early embryos (Fig. 3A,D), GFP-ZYG-11 levels are dramatically increased when *cul-2* is inactivated (Fig. 3B,E,G). As anticipated, analogous results were obtained after *elc-1* inactivation (Fig. 3G). Elevated levels of GFP-ZYG-11 do not result merely from slower progression through meiosis II, because GFP-ZYG-11 is not increased in *cyb-3*(*RNAi*) animals (Fig. 3C,F,G). These observations are compatible with ZYG-11 being a substrate recruitment subunit of a CUL-2 containing ECS ligase.

We next addressed whether *zyg-11* is required for the activity of all ECS complexes. ZIF-1 is the SOCS-box protein of an ECS that targets germ plasm proteins for degradation in

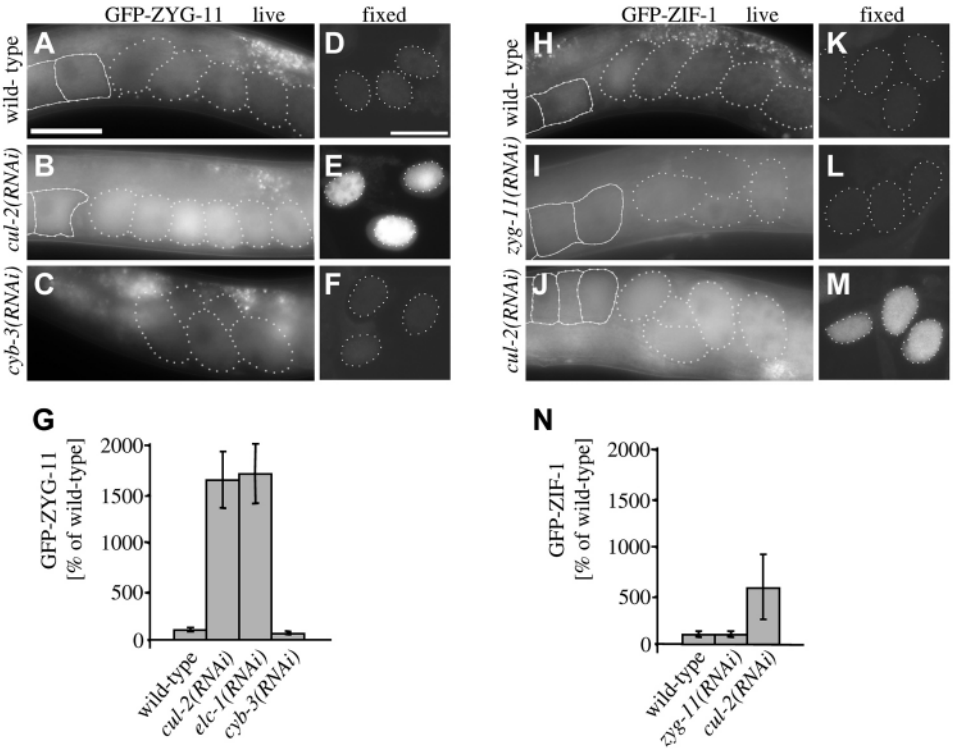

Fig. 3. *cul-2* destabilizes GFP-ZYG-11; *zyg-11* does not regulate GFP-ZIF-1. Images of paralyzed animals (A-C,H-J) or of fixed embryos stained with anti-GFP antibodies (D-F,K-M) from strains expressing GFP-ZYG-11 (A-F) or GFP-ZIF-1 (H-M). Plain outlines indicate oocytes, stippled outlines embryos. Note also the gut autofluorescence outside of embryos in live specimens. Scale bars: 50 μm. (G,N) Quantification of GFP-ZYG-11 (G) and GFP-ZIF-1 (N) signal intensities in fixed early embryos (i.e. <10 cell stage) of the indicated genotypes stained as in (D-F,K-M). Increase of GFP-ZYG-11 in *cul-2*(*RNAi*) is 16.4±3.0-fold, of GFP-ZYG-11 in *elc-1*(*RNAi*) is 17.3±3.2-fold, and of GFP-ZIF-1 in *cul-2*(RNAi) is 5.8±3.3-fold.

somatic lineages in early embryos (DeRenzo et al., 2003). In *cul-2*(*RNAi*) animals, levels of GFP-ZIF-1 are increased compared with otherwise wild-type embryos (Fig. 3H,J,K,M,N) (DeRenzo et al., 2003). By contrast, we found that levels of GFP-ZIF-1 are not altered in *zyg-11*(*RNAi*) animals (Fig. 3I,L,N). We conclude that *zyg-11* is not required for the function of all CUL-2-containing E3 ligases but plays a more restricted role during meiosis.

zyg-11 and *cul-2* function redundantly with APC during meiosis I

In addition to an essential requirement at meiosis II, we uncovered a non-essential function for *zyg-11* and *cul-2* at meiosis I. The *mat-1* locus encodes the APC component Cdc27/APC3 and embryos from the conditional allele *mat-1*(*ax161*) raised at 25°C arrest at the metaphase to anaphase transition of meiosis I (Fig. 4A-C, Table 2) (Golden et al., 2000; Wallenfang and Seydoux, 2000). Such arrested embryos fall into three categories on the basis of their position with respect to the spermatheca in the animal (data not shown), and the appearance of chromosomes and microtubules (Fig. 4). First, embryos closest to the spermatheca and thus the youngest, which have a canonical metaphase I arrest configuration (Fig. 4A, metaphase I). Second, embryos located further away from the spermatheca, which have chromosomes with a looser arrangement and a less organized spindle (Fig. 4B, metaphase I late). Third, embryos located further still from the spermatheca and thus the oldest, which have elongated chromosomes located in the embryo center and a completely disassembled spindle (Fig. 4C, metaphase I very late).

Although 15°C *mat-1*(*ax161*) embryos are indistinguishable from wild type (Fig. 4G,K,L; Table 2) (Golden et al., 2000; Wallenfang and Seydoux, 2000), we found that they exhibit meiosis I defects when, in addition, either *zyg-11* or *cul-2* are inactivated, accumulating with chromosomes and spindle configurations resembling those of 25°C *mat-1*(*ax161*) embryos (Fig. 4H-J, compare with Fig. 4A-C; Table 2). Although some 15°C *mat-1*(*ax161*) *zyg-11*(*RNAi*) and 15°C *mat-1*(*ax161*) *cul-2*(*RNAi*) embryos bypass the meiosis I block, the first polar body is small or absent (data not shown) and metaphase II figures invariably exhibit supernumerary chromosomes, which is indicative of defective anaphase I (Fig. 4M,N). Similar results were obtained using a distinct conditional *mat-1* allele, *mat-1*(*ax144*) (Table 2). These findings indicate that *zyg-11* and *cul-2* also act at meiosis I, although this role is revealed only when APC function is slightly compromised. Because *zyg-11* behaves like *cul-2* in enhancing the *mat-1* phenotype, these findings also reinforce the notion that ZYG-11 and CUL-2 function in a common process.

Interestingly, we noted that a sizeable fraction of 15°C *mat-1*(*ax161*) *zyg-11*(*RNAi*) and 15°C *mat-1*(*ax161*) *cul-2*(*RNAi*) metaphase II embryos have elongated chromosomes located in the center of the embryo and a completely disassembled spindle (Fig. 4O, Table 2), resembling the last category of 25°C *mat-1*(*ax161*) embryos (see Fig. 4C). Such configurations are never observed when *zyg-11* and *cul-2* are inactivated on their own (Fig. 2). Therefore, it appears that some embryos lacking *zyg-11* or *cul-2* function cannot exit meiosis II if APC function is compromised. Although this may be a consequence of the meiosis I defects, it could also reflect a requirement for APC at meiosis II.

Inverted polarity is established during the meiosis II delay in the absence of *zyg-11* or *cul-2* function

Next, we investigated the cause of the alterations in cleavage

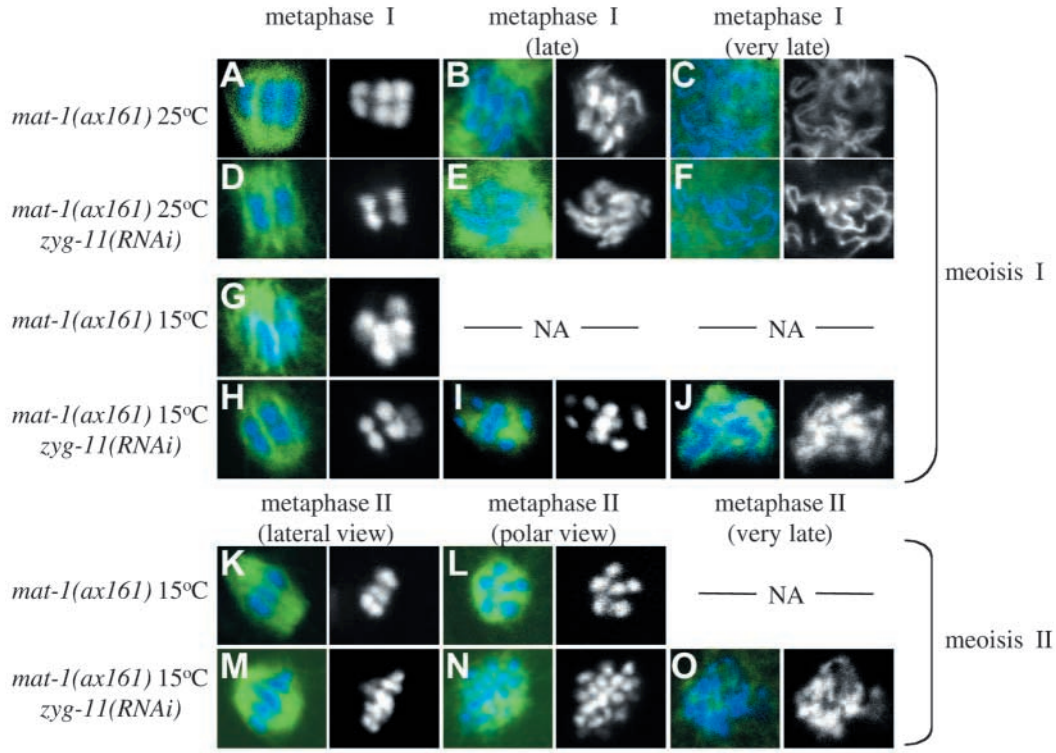

Fig. 4. *zyg-11* and *cul-2* function redundantly with APC at meiosis I. Meiotic figures from embryos of the indicated genotypes stained with antibodies against α-tubulin (green in merge) are shown; DNA is shown in blue in merged image and alone on the right. Width of panel represents ~7 μm. NA, not available.

pattern and P granule distribution that have been reported in *zyg-11*(*mn40*) embryos (Kemphues et al., 1986) by analyzing the distribution of polarity markers. In wild-type meiosis II, PAR-1, PAR-2 and PAR-3 proteins are not polarized, and P-granules are present throughout the cytoplasm (Fig. 5A-D, Table 3). By contrast, we found that ~50% of *zyg-11(RNAi)* meiosis II embryos exhibit polarized distribution of PAR proteins and P-granules (Fig. 5E-H, Table 3), although enrichment of all four markers is typically less pronounced than for wild-type embryos during the first mitotic cell cycle (Fig. 5Q-T). Strikingly, in all *zyg-11(RNAi)* meiosis II embryos with polarized distribution, PAR-1, PAR-2 and P-granules are enriched in the vicinity of the meiotic spindle, whereas PAR-3 is enriched on the opposite side. These distributions are inverted compared with wild-type embryos during the first mitotic cell cycle. We next examined *cul-2*(*RNAi*) meiosis II embryos and found similar alterations in the distribution of PAR-1, PAR-2, PAR-3 and P granules (Fig. 5I-L, Table 3). We conclude that inverted polarity is established during meiosis II in the absence of *zyg-11* or *cul-2* function.

zyg-11 and *cul-2* prevent polarity establishment independently of promoting meiosis II cell cycle progression

Inverted polarity could be a consequence of prolonged meiosis II or reflect a more direct requirement of *zyg-11* and *cul-2* to negatively regulate polarity establishment. To distinguish between these possibilities, we first examined the distribution of polarity markers in *cyb-3*(*RNAi*) embryos, which also exhibit delayed progression through meiosis II (Fig. 1 and Table S1). Importantly, we found that PAR-1, PAR-2, PAR-3 and P granules are not polarized in *cyb-3*(*RNAi*) meiosis II

Table 2. *zyg-11* and *cul-2* act redundantly with APC at meiosis I

	n	Metaphase I	Metaphase I (late)	Metaphase I (very late)	Metaphase II	Metaphase II (very late)	All older embryos
mat-1(ax161) 25°C	130	25%	46%	29%	–	–	–
mat-1(ax161) 25°C; *zyg-11(RNAi)*	184	28%	49%	23%	–	–	–
mat-1(ax161) 25°C; *cul-2(RNAi)*	156	24%	47%	29%	–	–	–
mat-1(ax161) 15°C	168	11%*	–	–	8%*	–	81%
mat-1(ax161) 15°C; *zyg-11(RNAi)*	153	25%	18%	1%	37%	12%	5%
mat-1(ax161) 15°C; *cul-2(RNAi)*	106	21%	14%	6%	32%	19%	8%
mat-1(ax144) 15°C	137	15%*	–	–	9%*	–	75%
mat-1(ax144) 15°C; *zyg-11(RNAi)*	108	10%	14%	3%	25%	10%	38%
mat-1(ax144) 15°C; *cul-2(RNAi)*	129	13%	16%	1%	19%	13%	39%

Fixed embryos of the indicated genotypes were placed into a category based on the status of chromosome configurations (see Fig. 4). Although often lacking a first polar body, meiosis II *mat-1*(*ax161*) *zyg-11*(*RNAi*) and *mat-1*(*ax161*) *cul-2*(*RNAi*) embryos raised at 15°C were unambiguously recognized because they are slightly smaller (being separated from the eggshell), have smaller chromosomes, and have a more intact cortex after fixation and staining than meiosis I embryos.

*For convenience of display, the metaphase I and metaphase II categories for *mat-1* mutant embryos at 15°C include anaphase I and anaphase II, respectively.

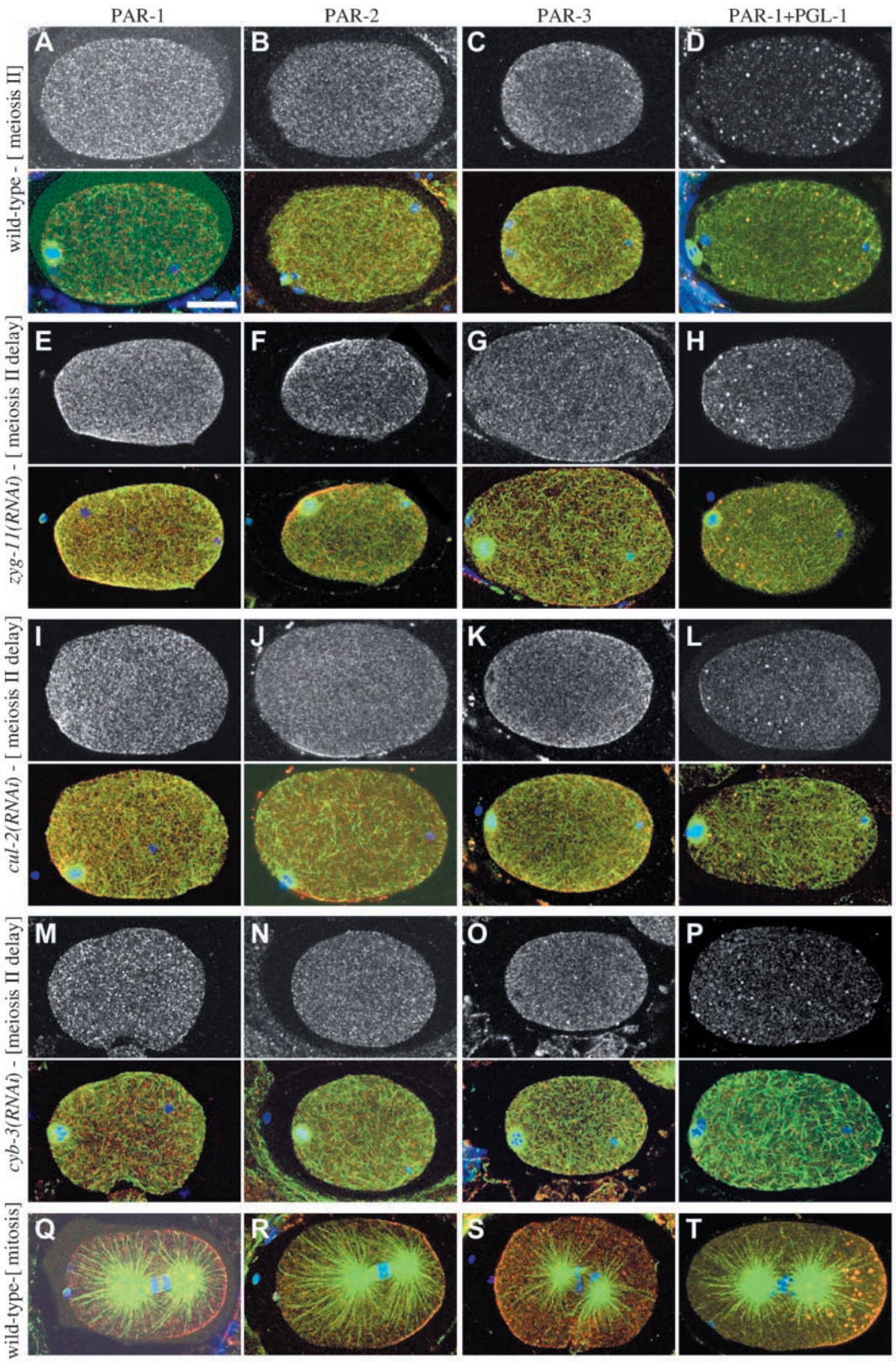

Fig. 5. Inverted AP polarity during meiosis II delay in the absence of *zyg-11* or *cul-2* function. Wild-type (A-D), *zyg-11*(*RNAi*) (E-H), *cul-2*(*RNAi*) (I-L), and *cyb-3*(*RNAi*) (M-P) embryos during meiosis II, and wild-type embryos during the first mitotic cell cycle (Q-T), stained with antibodies against α-tubulin (green in merged image) and a polarity marker as indicated (PAR-1, PAR-2, PAR-3 or PAR-1+PGL-1 to detect P granules; red in merged image and viewed alone in the top panel); DNA is shown in blue in merged image. Scale bar: 10 μm. Note that enrichment of PAR proteins and P granules in the absence of *zyg-11* or *cul-2* function is somewhat variable during meiosis II, and is less pronounced, both in intensity and in lateral extent, than in wild-type embryos during the first mitotic cell cycle.

Table 3. Distribution of polarity markers following *zyg-11*, *cul-2* or *cyb-3* inactivation

	Meiosis II delay			First mitotic cell cycle				First cleavage pattern: Two-cell stage			
	inv.	not loc.	*n*	inv.	not loc.	wt	*n*	inv.	sym.	wt	*n*
PAR-1											
zyg-11(RNAi)	51%	49%	65	27%	13%	60%	30	36%	15%	49%	53
cul-2(RNAi)	40%	60%	42	38%	24%	38%	42	42%	16%	42%	50
cyb-3(RNAi)	0%	100%	18	0%	0%	100%	20	0%	0%	100%	54
zyg-11(RNAi); spd-2(oj29)	52%	48%	33	75%	15%	10%	20	60%	21%	19%	43
PAR-2											
zyg-11(RNAi)	58%	42%	60	28%	16%	56%	25				
cul-2(RNAi)	71%	29%	117	31%	23%	46%	13				
cyb-3(RNAi)	3%*	97%	38	0%	0%	100%	51				
PAR-3											
zyg-11(RNAi)	49%	51%	45	18%	43%	39%	28				
cul-2(RNAi)	44%	56%	32	27%	19%	54%	26				
cyb-3(RNAi)	0%	100%	26	3%	0%	97%	31				
PGL-1											
zyg-11(RNAi)	55%	45%	60			mislocalized†					
cul-2(RNAi)	67%	33%	117			mislocalized†					
cyb-3(RNAi)	0%	100%	10	0%	0%	100%	10				

Fixed embryos of the indicated genotypes stained with antibodies against α-tubulin and PAR-1, PAR-2, PAR-3 or PGL-1, and counterstained with Hoechst to view DNA, were analyzed during the meiosis II delay and the first mitotic cell cycle. Moreover, the cleavage pattern was determined in embryos stained with PAR-1. Some embryos were stained simultaneously with PAR-2 and PGL-1; all embryos with inverted P granule localization also exhibited inverted PAR-2. inv., inverted compared with the situation in wild type during the first mitotic cell cycle; not loc., not localized.

Indicated also is whether the first cleavage was inverted compared with wild type (inv.), was symmetric (sym.) or was as in wild type (wt).

*In one *cyb-3*(*RNAi*) embryo, PAR-2 was detected at both poles.

†P granules were typically more concentrated in the vicinity of the two poles.

embryos (Fig. 5M-5P), indicating that the inverted polarity established in *zyg-11*(*RNAi*) or *cul-2*(*RNAi*) embryos is unlikely to result merely from prolonged meiosis II.

Because the meiosis II delay in *cyb-3*(*RNAi*) embryos is slightly less pronounced and of a different nature than that observed in *zyg-11*(*RNAi*) or *cul-2*(*RNAi*) embryos, we conducted two experiments to test whether *zyg-11* and *cul-2* can regulate polarity establishment independently of their requirement for cell cycle progression during meiosis II. First, we made use of 25°C *mat-1*(*ax161*) embryos, which are arrested in meiosis I with evenly distributed P granules (Fig. 6A,B, Table 4) (Wallenfang and Seydoux, 2000). Because P granules are polarized in an inverted manner in ~50% of embryos lacking *zyg-11* or *cul-2* function (Table 3), we performed a molecular epistasis experiment using 25°C *mat-1*(*ax161*) embryos subjected to *zyg-11*(*RNAi*) or *cul-2*(*RNAi*). Interestingly, we found that ~30% of 25°C *mat-1*(*ax161*) embryos lacking, in addition, either *zyg-11* or *cul-2* function, exhibit an enrichment of P granules in the vicinity of the meiotic spindle (Fig. 6D, Table 4). Because the CUL-2-based E3 ligase plays a non-essential role at meiosis I, we considered whether this may reflect a more robust cell cycle arrest in such embryos. However, we found that the fraction of embryos in each of the three meiosis I arrest categories (Fig. 4) is the same in 25°C *mat-1*(*ax161*) embryos irrespective of whether they have been subjected to *zyg-11*(*RNAi*) or *cul-2*(*RNAi*) (Table 2), indicating that cell cycle progression is similarly affected.

In a second experiment, we made use of *ncc-1*(*RNAi*) embryos. *ncc-1* encodes a *Cdc2* kinase acting during meiosis; in its absence, chromosomes do not congress to form a metaphase plate and both meiotic divisions fail (Boxem et al., 1999). Nevertheless, the time interval between fertilization and the appearance of pronuclei is unchanged as the meiotic divisions are bypassed (Boxem et al., 1999). We found the average number of embryos in meiosis, as judged by examining chromosomes with GFP-HIS, to be 1.5/gonad for *ncc-1*(*RNAi*) (*n*=17 gonads), 3.0/gonad for *zyg-11*(*mn40*) (*n*=23 gonads) and 1.6/gonad for *ncc-1*(*RNAi*) *zyg-11*(*mn40*) (*n*=25 gonads). This indicates that the time separating fertilization from pronuclear appearance is not changed in *zyg-11*(*mn40*) *ncc-1*(*RNAi*) embryos compared with *ncc-1*(*RNAi*) embryos, enabling us to test the requirement of *zyg-11* in polarity establishment independently of that in meiotic cell cycle progression. As shown in Fig. 6F, we observed cortical enrichment of GFP-PAR-2 in the vicinity of oocyte chromosomes in ~60% of *zyg-11*(*mn40*) *ncc-1*(*RNAi*) embryos prior to pronuclear appearance (*n*=29), although to lower levels than in *zyg-11*(*mn40*) embryos (data not shown). Taken together, our findings indicate that *zyg-11* and *cul-2* can regulate polarity establishment independently of their requirement for meiosis II cell cycle progression.

Timing of inverted polarity establishment

We noted that only 25°C *mat-1*(*ax161*) *zyg-11*(*RNAi*) or 25°C *mat-1*(*ax161*) *cul-2*(*RNAi*) embryos of the ‘metaphase I late’ and ‘metaphase I very late’ categories show polarized distribution of P granules (Fig. 6D; Table 4). Compatible with this view, inverted distribution of GFP-PAR-2 in *mat-1*(*RNAi*) or *mat-1*(*RNAi*) *zyg-11*(*mn40*) embryos is found predominantly in embryos of these two categories (Fig. 6H,J; Table 4). Therefore, inverted polarity is established some time after the initial metaphase I arrest in embryos lacking both *mat-1* and *zyg-11* function.

By analogy, we considered whether inverted polarity might

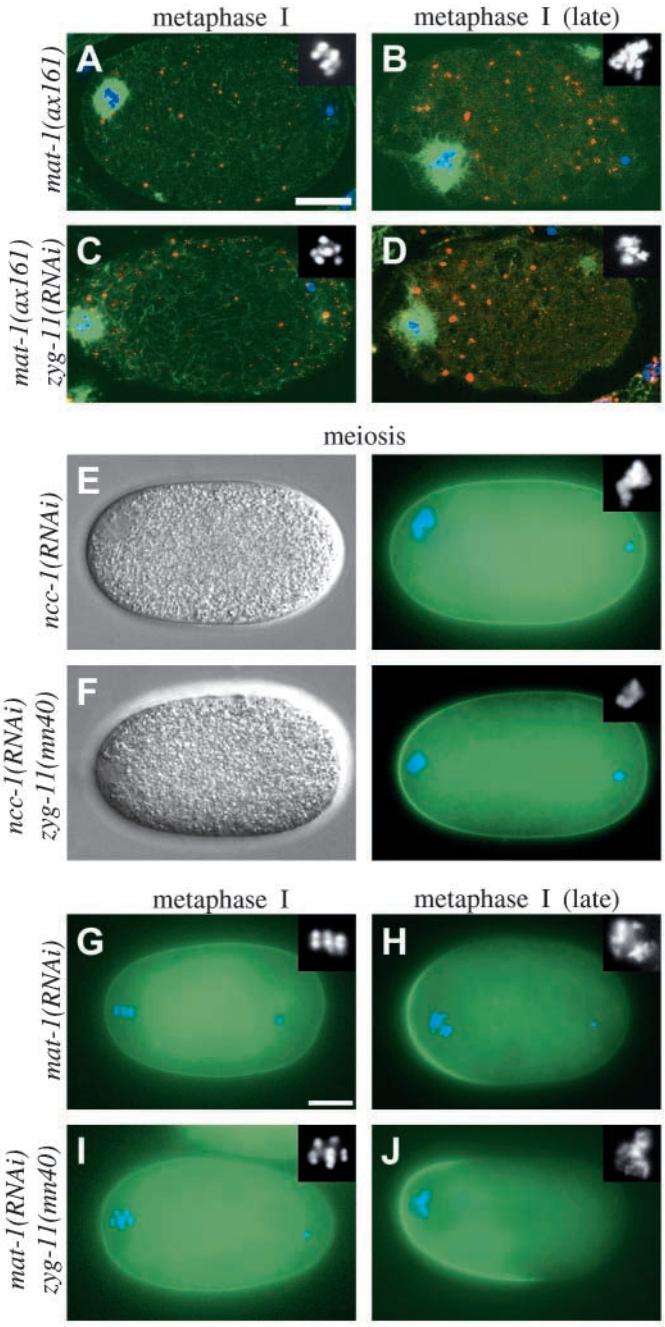

Fig. 6. *zyg-11* can prevent polarity establishment independently of promoting meiosis II cell cycle progression. (A-D) 25°C *mat-1*(*ax161*) or 25°C *mat-1*(*ax161*) *zyg-11*(*RNAi*) embryos stained with antibodies against α-tubulin (green) and PGL-1 to detect P granules (red); DNA is shown in blue. Depicted are embryos from the metaphase I (A,C) and the metaphase I (late) (B,D) categories (see Fig. 4). Insets show magnified views of meiotic chromosomes. Scale bar: 10 μm; width of inset represents ~7 μm. (E,F) Live *ncc-1*(*RNAi*) [heterozygous for *zyg-11*(*mn40*)] or *ncc-1*(*RNAi*) *zyg-11*(*mn40*) embryos during meiosis expressing GFP-PAR-2 (green) and stained with Hoechst 33342 to view DNA (blue in merged image). Insets show magnified views of meiotic chromosomes; width of inset represents ~8 μm. Left panels show a DIC image of the same embryo. (G-J) Live *mat-1*(*RNAi*) [heterozygous for *zyg-11*(*mn40*)] or *mat-1*(*RNAi*) *zyg-11*(*mn40*) embryos expressing GFP-PAR-2 (green) and stained with Hoechst 33342 to view DNA (blue in merged image). Insets show magnified views of meiotic chromosomes; width of inset represents ~8 μm. Scale bar: 10 μm.

be established some time after the initial metaphase II block in embryos lacking *zyg-11* or *cul-2* function. We imaged GFP-PAR-2 in *zyg-11*(*RNAi*) and *zyg-11*(*mn40*) embryos, and found that cortical enrichment in the vicinity of the meiotic spindle always becomes apparent during the second half of the delay (Fig. 1B, vertical white lines; *n*=7). This is likely to explain why polarity inversion is observed in ~50% of fixed *zyg-11*(*RNAi*) or *cul-2*(*RNAi*) meiosis II embryos, and indicates that inverted polarity is invariably established by the end of the meiotic cell cycle in the absence of *zyg-11* or *cul-2* function.

Plasticity of polarity after the meiotic cell cycle in *zyg-11*(*RNAi*) embryos

We next investigated how polarity inversion by the end of meiosis II generates the diverse cleavage patterns that occur in the absence of *zyg-11* function (Kemphues et al., 1986). By live imaging of *zyg-11*(*RNAi*) embryos expressing GFP-HIS and GFP-PAR-2, we found that a second GFP-PAR-2 domain, which is variable in size, is always established on the opposite side of the embryo at the onset of the first mitotic cell cycle, as in wild type (see Movies 8-10 at http://dev.biologists.org/supplemental/; *n*=19). Therefore, *zyg-11*(*RNAi*) embryos experience two polarizing signals, one during meiosis II and a second one at the onset of the first mitotic cell cycle.

We found that these embryos can be placed into three classes according to the evolution of the two GFP-PAR-2 domains. In six embryos, the first GFP-PAR-2 domain diminishes in

Table 4. *zyg-11* and *cul-2* can prevent polarity establishment independently of promoting meiosis II cell cycle progression

	Metaphase I			Metaphase I (late)			Metaphase I (very late)		
	inv.	not loc.	*n*	inv.	not loc.	*n*	inv.*	not loc.	*n*
PGL-1									
mat-1(ax161) 25°C	0%	100%	41	0%	100%	20	0%	100%	9
mat-1(ax161) 25°C; *zyg-11(RNAi)*	0%	100%	48	80%	20%	35	27%	73%	11
mat-1(ax161) 25°C; *cul-2(RNAi)*	0%	100%	32	71%	29%	17	33%	67%	6
GFP-PAR-2									
mat-1(RNAi)	14%	86%	21	97%	3%	37	24%	76%	41

Fixed embryos of the indicated genotypes were placed into a category based on the status of chromosome configurations (see Fig. 4), and analyzed for PGL-1 distribution. Live *mat-1*(*RNAi*) embryos expressing GFP-PAR-2 and stained with Hoechst 33342 were also analyzed. inv., inverted compared with the situation in wild type during the first mitotic cell cycle (although enriched to a lesser extent); not loc., not localized.

*P granules are enriched in the proximity of oocyte-derived chromosomes, which are located in the cell center of embryos in this category.

intensity, whereas the second one becomes more robust; embryos in this first class divide asymmetrically as in wild type, yielding a smaller blastomere on the side of the prevailing GFP-PAR-2 domain (Fig. 7A,D; see Movie 8 at http://dev.biologists.org/supplemental/). In 10 embryos, the first GFP-PAR-2 domain remains robust, whereas the second one diminishes in intensity; embryos in this second class divide asymmetrically, but in an inverted manner compared with wild type (Fig. 7B,D; Movie 9 at http://dev.biologists.org/supplemental/). In the remaining three embryos, both domains of GFP-PAR-2 become undetectable by the end of the first mitotic cell cycle; embryos in this third class divide symmetrically (Fig. 7C,D; Movie 10 at http://dev.biologists.org/supplemental/). These findings suggest that one PAR-2-containing domain at most can be present by the end of the first mitotic cell cycle and that this domain is predictive of spindle positioning during the first cleavage division.

We used GFP-HIS to follow sperm-derived chromosomes in the three classes of *zyg-11*(*RNAi*) embryos (*n*=14). In the first class, where the second GFP-PAR-2 domain prevails, sperm chromosomes remain in the position they occupy in wild type, opposite the first GFP-PAR-2 domain (Movie 8 at http://dev.biologists.org/supplemental/; 6/6 embryos). In most embryos of the second class, where the first GFP-PAR-2 domain prevails, sperm chromosomes are initially in their normal position, but then move towards the inverted GFP-PAR-2 domain (Movie 9 at http://dev.biologists.org/supplemental/; 5/6 embryos). In the third class, where both GFP-PAR-2 domains become undetectable, sperm chromosomes are also initially in their normal position, but then move towards the cell center (Movie 10 at http://dev.biologists.org/supplemental/; 2/2 embryos). These observations suggest that the cleavage pattern of *zyg-11*(*RNAi*) embryos is dictated primarily by the position of a sperm-derived component during the course of the first mitotic cell cycle.

To test this hypothesis further, we analyzed polarity in embryos lacking both *zyg-11* and *spd-2*, which is required for establishing polarity induced by the sperm-derived component (O'Connell et al., 2000). We found that *spd-2* is dispensable for establishing inverted polarity in the absence of *zyg-11* at meiosis II, as PAR-1 is still inverted in ~50% of fixed *spd-2*(*oj29*) *zyg-11*(*RNAi*) meiosis II embryos (Table 3). In addition, the fraction of embryos with an inverted first division is increased from 36% in *zyg-11(RNAi)* embryos to 60% in *zyg-11(RNAi) spd-2(oj29)* (Table 3). These findings indicate that a sperm-derived component that is in part *spd-2* dependent competes with the inverted polarity established during the meiosis II delay to result in a single GFP-PAR-2 domain by the end of the first mitotic cell cycle.

Microtubules and polarity establishment during meiosis II and the first mitotic cell cycle

We next investigated whether establishment of inverted polarity during the meiotic II delay is microtubule dependent. We eliminated microtubules from *zyg-11*(*mn40*) mutant embryos using RNAi against the alpha tubulin gene *tba-2*, thus likely inactivating all alpha tubulin genes owing to cross-RNAi between highly related sequences (Wright and Hunter, 2003). In such embryos, all microtubule processes, including the two meiotic divisions, are defective, and all oocyte chromosomes are found approximately two-thirds of the way down the length of the egg (Yang et al., 2003) (Fig. 8B and data not shown). Importantly, we found that ~65% of *zyg-11*(*mn40*) *tba-2*(*RNAi*) meiosis II embryos have a patch of cortical GFP-PAR-2 (Fig. 8B; *n*=18), which is comparable to the fraction of *zyg-11*(*RNAi*) meiosis II embryos exhibiting inverted PAR-2 cortical localization (Table 3). Similar findings were made examining PAR-1 distribution (data not shown). Moreover, P granules tend to be enriched in the vicinity of cortical GFP-PAR-2 (Fig. 8B). Interestingly, we noted also that the patch of

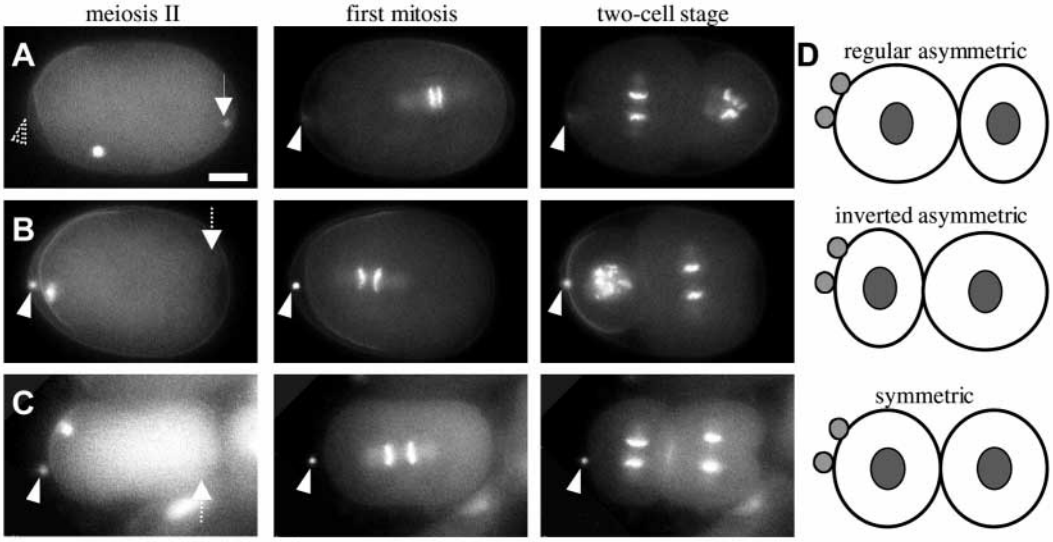

Fig. 7. Evolution of polarity in *zyg-11*(*RNAi*) embryos. (A-C) Images from time-lapse sequences of *zyg-11*(*RNAi*) embryos expressing GFP-PAR-2 and GFP-HIS, as well as GFP-TUB, shown during the meoisis II delay (left panel), the first mitotic division (middle panel) and the two- to four-cell stage transition (right panel) (see also movies 8-10 at http://dev.biologists.org/supplemental/). Recordings were started during the meiosis II delay. Arrowheads point to first polar body, arrows indicate condensed sperm DNA; stippled arrowhead and arrows indicate that these positions can be determined only from the movies. Scale bar: 10 μm. (D) Schematic representation of two-cell stage embryos (*n*=19) corresponding to recordings A (6 embryos), B (10 embryos) or C (3 embryos). See text for details.

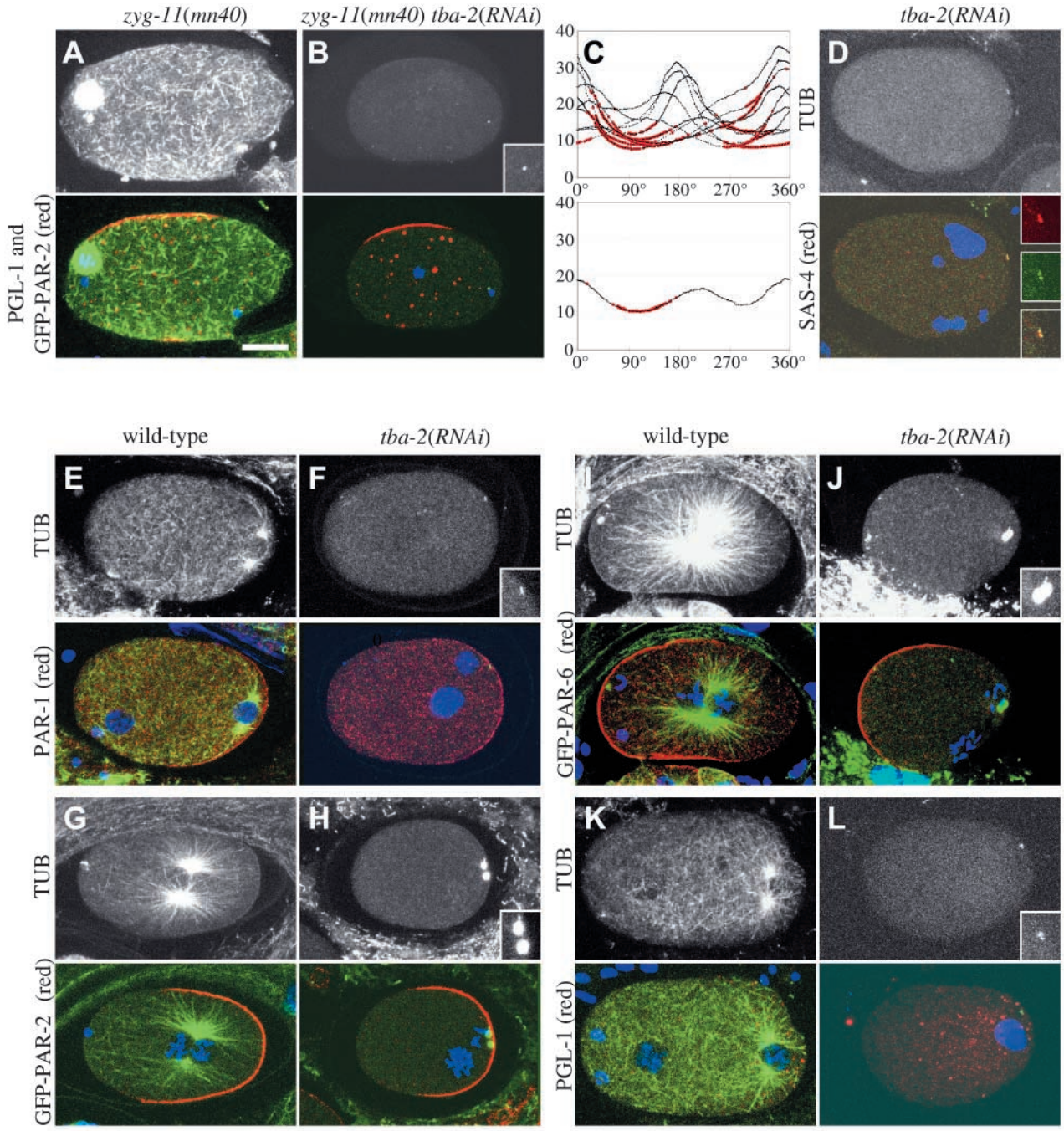

Fig. 8. Establishment of AP polarity occurs independently of astral microtubules. *zyg-11*(*mn40*) (A) or *zyg-11*(*mn40*) *tba-2*(*RNAi*) (B) meiosis II embryos, wild-type (E,G,I,K) or *tba-2*(*RNAi*) embryos (F,H,J,L) during the first mitotic cell cycle, and *tba-2*(*RNAi*) embryos during the second mitotic cell cycle (D) are shown. All embryos are stained with antibodies against α-tubulin (green in merged image) and a centriolar or polarity marker as indicated (SAS-4, PAR-1, GFP-PAR-2, GFP-PAR-6, PGL-1; red in merged image); DNA is shown in blue in the merged image. A dozen ~1 μm confocal optical sections were imaged. The top panels show a projection of all slices for the α-tubulin channel. Insets show magnified views of centrosomes; width of inset represents ~5 μm. The merged images show a single section for α-tubulin and the centriolar or polarity marker, along with a projection of all slices for the DNA signal. Scale bar: 10 μm. (C) Plots of position along the circumference in *zyg-11*(*mn40*) *tba-2*(*RNAi*) embryos (*x*-axis, degrees, with 0 degrees being posterior-most) as a function of the distance separating oocyte chromosomes from the cortex (*y*-axis, μm). Red dots indicate cortical locations where GFP-PAR-2 levels are at least five times higher than in the cytoplasm (determined with Metamorph software). Top plot, ten embryos; bottom plot, embryo shown in B. Note that GFP-PAR-2 is present in the cortical region closest to oocyte chromosomes. (E-L) Pairs of wild-type and *tba-2*(*RNAi*) embryos, from approximately the same stage, during prophase of the first cell cycle. In all *tba-2*(*RNAi*) embryos lacking detectable astral microtubules, including those with only two tiny dots of α-tubulin presumably corresponding to paternally contributed centrioles (F,L, see also D), polarity markers were distributed as in wild type [number of embryos examined for each polarity marker (the number of embryos that only have two tiny dots is given in parentheses): PAR-1, 10 (5); GFP-PAR-2, 6 (1); GFP-PAR-6, 6 (0); PGL-1, 10 (5)].

GFP-PAR-2 is located invariably on the cortex closest to oocyte chromosomes (Fig. 8C), raising the possibility that they may somehow influence positioning of cortical GFP-PAR-2. Together, these observations indicate that microtubules are not essential for imparting ectopic polarity in the absence of *zyg-11* function.

These results raise the possibility that microtubules may also not be essential for establishing AP polarity during the first mitotic cell cycle. To test whether this is the case, we examined markers of polarity in *tba-2*(*RNAi*) embryos. Cortical, astral and spindle microtubules are not detected in one-cell stage *tba-2*(*RNAi*) embryos, and the sole remnant of the microtubule cytoskeleton is the centrosome, presumably because it is the favoured site of microtubule nucleation for any tubulin dimers remaining after RNAi treatment (Fig. 8F,H,J,L). In severely affected embryos, only two tiny dots are observed, which co-localize with the centriolar protein SAS-4 (Fig. 8D), indicating that they correspond to paternally contributed centrioles. Strikingly, we found that PAR-1, GFP-PAR-2, GFP-PAR-6 and P granules always localize correctly in *tba-2*(*RNAi*) embryos during the first mitotic cell cycle (Fig. 8E-L). Furthermore, the onset of polarized distribution is comparable to that of wild-type embryos; for instance, PAR-1 and P granules enrichments begin during early prophase. The same conclusion is reached with live imaging of *tba-2*(*RNAi*) embryos expressing GFP-PAR-2 and GFP-PAR-6 (data not shown). Therefore, microtubules appear not to be necessary for establishing AP polarity in one-cell stage *C. elegans* embryos.

Discussion

A novel CUL-2-based E3 ligase acting in early *C. elegans* embryos

The molecular nature of ZYG-11 does not offer immediate clues as to its mode of action. Our analysis, together with the accompanying work by Liu et al. (Liu et al., 2004), reveals that *zyg-11* is likely to act with a CUL-2-containing E3 ligase at meiosis. Could ZYG-11 be a substrate of this ECS, given that GFP-ZYG-11 levels are dramatically increased in the absence of *cul-2*? This possibility seems unlikely, given that inactivation of the ECS and of its substrate are expected to yield opposite, not identical, phenotypes. Although other scenarios can be envisaged, a plausible hypothesis is that ZYG-11 is the substrate recruitment component of this ECS. Although this seems at odds with the fact that ZYG-11 does not contain a recognizable SOCS box, this motif can be very divergent, as is the case for ZIF-1 (DeRenzo et al., 2003), and *Drosophila* Zyg11 contains a potential SOCS box (R.S. and P.G., unpublished). Whether *C. elegans* ZYG-11 truly acts as a substrate recruitment subunit remains to be ascertained biochemically.

Regulated protein degradation by way of E3 ligases plays a crucial role in other aspects of early *C. elegans* development. Another ECS that uses ZIF-1 as a substrate recruitment subunit is essential for removing several CCCH finger proteins from somatic lineages (DeRenzo et al., 2003). Moreover, a CUL-3-based complex is essential for degradation of the meiosis-specific microtubule-severing protein MEI-1 during the first mitotic cell cycle (Kurz et al., 2002; Pintard et al., 2003a). The activity of these two E3 ligases is dependent on the DYRK kinase MBK-2 (Pellettieri et al., 2003). This does not seem to be the case for the ECS described in this work, as embryos lacking *mbk-2* function complete the meiotic divisions normally and have no apparent polarity defects (Pellettieri et al., 2003).

The APC and an ECS together ensure progression through the two meiotic divisions

Previous work established that the APC is essential for the metaphase to anaphase transition of meiosis I in *C. elegans* (Golden et al., 2000; Wallenfang and Seydoux, 2000). Hypomorphic APC mutants that affect meiosis I without arresting cell cycle progression exhibit defective sister chromatid segregation at meiosis II (Shakes et al., 2003). However, this may result from the aberrant meiosis I, as no semi-permissive conditions were found that yield a meiosis II arrest, raising the possibility that APC is not required at meiosis II (Shakes et al., 2003). Compatible with this view, the APC component FZY-1 localizes to chromosomes during meiosis I but not meiosis II (Kitagawa et al., 2002). Here, we establish that a CUL-2-based E3 ligase is required for progression through meiosis II. Though unlikely given the distinct phenotypes of APC hypomorphic mutants and of *zyg-11* or *cul-2* inactivation, the possibility that this ECS is an essential positive regulator of the APC cannot be excluded for meiosis II. By contrast, this cannot be the case at meiosis I, because inactivation of *zyg-11* or *cul-2* does not affect meiosis I, whereas that of the APC results in metaphase I arrest. Although embryos lacking *zyg-11* or *cul-2* do not arrest at meiosis I, compromising APC activity slightly in these embryos results in meiosis I defects, indicating that the ECS plays a non-essential role at meiosis I.

Interestingly, progression through the meiotic cell cycle in other organisms also rests on distinct E3 ligases at meiosis I and meiosis II. In *Saccharomyces pombe*, the Fizzy/Cdc20-related APC activator mfr1 is required specifically at meiosis II for degradation of the B-type cyclin cdc13 (Blanco et al., 2001). Similarly, in *Drosophila*, the Cdc20/Fizzy protein Cortex is required for timely metaphase to anaphase transition at meiosis II (Chu et al., 2001; Page and Orr-Weaver, 1996). Thus, whereas meiosis II in *S. pombe* and *Drosophila* relies on specific APC variants, it requires the activity of an ECS in *C. elegans*.

What substrates of the CUL-2-based E3 ligase must be targeted for degradation to ensure progression through meiosis II in *C. elegans*? The metaphase to anaphase transition is generally triggered when securin is targeted for degradation. IFY-1 is a *C. elegans* destruction-box protein that has properties expected from a securin (Kitagawa et al., 2002), and it will be interesting to test whether the CUL-2-based E3 ligase mediates IFY-1 degradation at meiosis II. Furthermore, M phase exit is generally triggered when B type cyclins are targeted for degradation. Our findings that *cyb-3* inactivation prevents the anaphase delay of embryos lacking *zyg-11* function strongly suggests that CYB-3 is a target of the CUL-2-based E3 ligase at meiosis II.

zyg-11 and *cul-2* prevent polarity establishment

In wild type, the first signs of polarized GFP-PAR-2 distribution occur shortly after meiosis II. Whether polarity is established when a set time is reached (e.g. after fertilization), or when a given cell cycle stage is encountered, has not been

addressed prior to this work. We found that asymmetric distribution of polarity markers in *cyb-3*(*RNAi*) embryos is not established during the meiosis II delay, but instead during the first mitotic cell cycle (R.S. and P.G., unpublished). Therefore, polarity establishment does not occur at a fixed time after fertilization or meiosis I, but is coupled instead to exit from the meiotic cell cycle and the onset of the first mitotic cell cycle.

In contrast to the situation in *cyb-3*(*RNAi*) embryos, inverted polarity is established during the meiosis II delay in embryos lacking *zyg-11* or *cul-2* function. We show that *zyg-11* and *cul-2* can regulate polarity establishment independently of promoting progression through meiosis II, suggesting that there are distinct polarity substrates that must be degraded by the CUL-2-based E3 ligase to prevent polarity establishment during meiosis II. As inverted polarity is also observed in metaphase I-arrested embryos lacking APC function (Wallenfang and Seydoux, 2000), it is tempting to speculate that at least some of these polarity substrates are shared between the two E3 ligases.

Interestingly, *cortex* mutant embryos in *Drosophila* have impaired polyadenylation of *bicoid* and *Toll* mRNAs, resulting in inefficient translation and ensuing defective embryonic polarity (Lieberfarb et al., 1996). Although the mechanisms by which APC promotes polyadenylation of these mRNAs remains to be clarified, it is remarkable that E3 ligases that ensure progression through meiosis II also serve to promote correct establishment of embryonic axes in diverse metazoan organisms.

Mechanisms of polarity establishment in *C. elegans*

It has been proposed that astral microtubules nucleated by the sperm aster are essential for establishing AP polarity in *C. elegans* embryos (O'Connell et al., 2000; Wallenfang and Seydoux, 2000). Our findings challenge this view. We establish that PAR-1, GFP-PAR-2, GFP-PAR-6, P granules and GFP-PIE-1 (R.S. and P.G., unpublished) all localize correctly in the first mitotic cell cycle in *tba-2*(*RNAi*) embryos. These results raise the possibility that microtubules are dispensable for AP polarity.

We recognize that we cannot exclude that minute microtubules undetectable by immunofluorescence or damaged during fixation may play a role. Nevertheless, we note that embryos lacking *spd-2*, *air-1* or *spd-5* function, while exhibiting delayed microtubule nucleation compared with wild type, have a more extensive microtubule network than *tba-2*(*RNAi*) embryos do (Hamill et al., 2002; O'Connell et al., 2000; Schumacher et al., 1998; Wallenfang and Seydoux, 2000). How can these apparently discrepant observations be reconciled? In wild type, the onset of GFP-PAR-2 accumulation at the cortex coincides with that of GFP-TUB on asters, early in the cell cycle (Cuenca et al., 2003). It may be that, at that early stage, minute microtubules are present in *tba-2*(*RNAi*) embryos, but not in embryos lacking *spd-2*, *air-1* or *spd-5* function. If this were the case, our findings would merely demonstrate that microtubules are dispensable for the expansion phase of the posterior PAR-2 cortical domain and not for the preceding initiation phase (Cuenca et al., 2003). However, we favour an alternative explanation in which microtubules are dispensable throughout the process, and in which *spd-2*, *air-1* and *spd-5* have a requirement for polarity establishment that is independent from their role in microtubule nucleation.

As sperm chromosomes are not essential for AP polarity (Sadler and Shakes, 2000), our findings lead us to suggest that, rather than astral microtubules, the sperm component acting as the polarity cue is the centrosome. Compatible with centrosomes being key, *spd-2*, *spd-5* and *air-1* are all required for centrosome maturation (Hamill et al., 2002; Hannak et al., 2001; O'Connell et al., 2000), and the corresponding proteins localize to the centrosome (Hamill et al., 2002; Schumacher et al., 1998; Hannak et al., 2001; Kemp et al., 2004). It will be interesting to investigate whether such a hypothetical polarity cue resides in centrioles or the surrounding pericentriolar

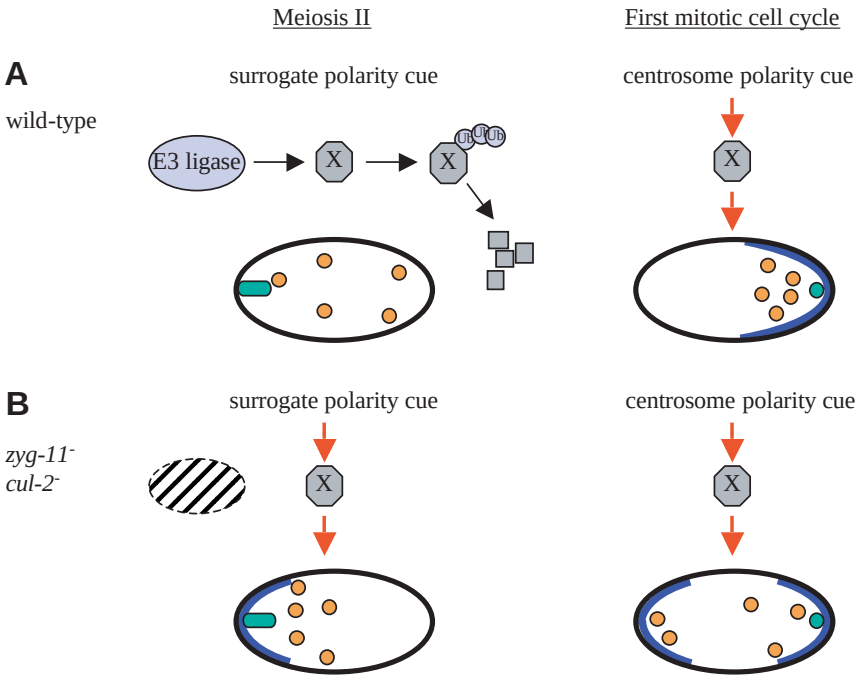

Fig. 9. Working model of polarity establishment in *C. elegans* embryos. (A) In wild-type meiosis II, a CUL-2-based E3 ligase that also requires *zyg-11* function ubiquitinates a substrate (X) that can induce polarity when triggered by a surrogate polarity cue, thus targeting the substrate for degradation by the proteasome. After exit from the meiotic cell cycle, E3 ligase activity is downregulated, allowing substrate accumulation and polarity establishment in response to the bona fide centrosome polarity cue. Green oval, oocyte chromosomes; green disk, centrosomes; blue crescent, cortical PAR-2; orange disks, P granules. Ubiquitin (Ub, blue circles) moieties are also shown. (B) In the absence of *zyg-11* or *cul-2*, substrate accumulation occurs during the meiotic cell cycle, resulting in polarity establishment in response to a surrogate polarity cue that correlates with the position of oocyte chromosomes. A related outcome may ensue when the APC is inactivated at meiosis I (not depicted here). After exit from the meiotic cell cycle in the absence of *zyg-11* or *cul-2*, a second focus of polarity is established in response to the centrosome polarity cue.

material. Equally interesting will be to elucidate how a component somehow correlated with the position of oocyte chromosomes, which do not have associated centrosomes, can act as a surrogate polarity cue during meiosis II.

Our findings taken together suggest a working model (Fig. 9) in which a CUL-2-based E3 ligase targets polarity substrates for degradation during meiosis II; as a result, polarity cannot be established. After exit from the meiotic cell cycle, polarity substrates accumulate, perhaps due to diminished E3 ligase activity, and thus the centrosome can induce polarity. We postulate that in the absence of *zyg-11* or *cul-2*, substrate accumulation occurs during the meiotic cell cycle, resulting in polarity establishment in response to a surrogate polarity cue.

For help in improving the manuscript, we thank Jean-Michel Bellanger, Ken Kemphues, Lionel Pintard and Viesturs Simanis. We are grateful to Ken Kemphues also for advice, encouragement, and *zyg-11* mutant alleles; to Michael Glotzer, Lionel Pintard, Geraldine Seydoux and Viesturs Simanis for reagents; to Edward Kipreos for communicating results prior to publication; and to Karine Baumer for generating transgenic lines. Some strains were obtained from the *Caenorhabditis* Genetics Center, which is funded by the NIH National Center for Research Resources (NCRR). This work was supported by grant 31-62102.00 from the Swiss National Science Foundation.

References

Blanco, M. A., Pelloquin, L. and Moreno, S. (2001). Fission yeast mfr1 activates APC and coordinates meiotic nuclear division with sporulation. *J. Cell Sci.* **114**, 2135-2143.

Boxem, M., Srinivasan, D. G. and van den Heuvel, S. (1999). The *Caenorhabditis elegans* gene *ncc-1* encodes a cdc2-related kinase required for M phase in meiotic and mitotic cell divisions, but not for S phase. *Development* **126**, 2227-2239.

Brauchle, M., Baumer, K. and Gönczy, P. (2003). Differential activation of the DNA replication checkpoint contributes to asynchrony of cell division in *C. elegans* embryos. *Curr. Biol.* **13**, 819-827.

Brenner, S. (1974). The genetics of *Caenorhabditis elegans*. *Genetics* **77**, 71-94.

Carter, P. W., Roos, J. M. and Kemphues, K. J. (1990). Molecular analysis of *zyg-11*, a maternal-effect gene required for early embryogenesis of *Caenorhabditis elegans*. *Mol. Gen. Genet.* **221**, 72-80.

Chu, T., Henrion, G., Haegeli, V. and Strickland, S. (2001). *Cortex*, a *Drosophila* gene required to complete oocyte meiosis, is a member of the Cdc20/fizzy protein family. *Genesis* **29**, 141-152.

Cuenca, A. A., Schetter, A., Aceto, D., Kemphues, K. and Seydoux, G. (2003). Polarization of the *C. elegans* zygote proceeds via distinct establishment and maintenance phases. *Development* **130**, 1255-1265.

DeRenzo, C., Reese, K. J. and Seydoux, G. (2003). Exclusion of germ plasm proteins from somatic lineages by cullin-dependent degradation. *Nature* **424**, 685-689.

Deshaies, R. J. (1999). SCF and Cullin/Ring H2-based ubiquitin ligases. *Annu. Rev. Cell. Dev. Biol.* **15**, 435-467.

Feng, H., Zhong, W., Punkosdy, G., Gu, S., Zhou, L., Seabolt, E. K. and Kipreos, E. T. (1999). CUL-2 is required for the G1-to-S-phase transition and mitotic chromosome condensation in *Caenorhabditis elegans*. *Nat. Cell Biol.* **1**, 486-492.

Fraser, A. G., Kamath, R. S., Zipperlen, P., Martinez-Campos, M., Sohrmann, M. and Ahringer, J. (2000). Functional genomic analysis of *C. elegans* chromosome I by systematic RNA interference. *Nature* **408**, 325-330.

Galan, J. M. and Peter, M. (1999). Ubiquitin-dependent degradation of multiple F-box proteins by an autocatalytic mechanism. *Proc. Natl. Acad. Sci. USA* **96**, 9124-9129.

Geyer, R., Wee, S., Anderson, S., Yates, J. and Wolf, D. A. (2003). BTB/POZ domain proteins are putative substrate adaptors for cullin 3 ubiquitin ligases. *Mol. Cell* **12**, 783-790.

Goh, P. Y. and Surana, U. (1999). Cdc4, a protein required for the onset of S phase, serves an essential function during G(2)/M transition in *Saccharomyces cerevisiae*. *Mol. Cell. Biol.* **19**, 5512-5522.

Golden, A., Sadler, P. L., Wallenfang, M. R., Schumacher, J. M., Hamill, D. R., Bates, G., Bowerman, B., Seydoux, G. and Shakes, D. C. (2000). Metaphase to anaphase (mat) transition-defective mutants in *Caenorhabditis elegans*. *J. Cell Biol.* **151**, 1469-1482.

Goldstein, B. and Hird, S. N. (1996). Specification of the anteroposterior axis in *Caenorhabditis elegans*. *Development* **122**, 1467-1474.

Gönczy, P., Schnabel, H., Kaletta, T., Amores, A. D., Hyman, T. and Schnabel, R. (1999). Dissection of cell division processes in the one cell stage *Caenorhabditis elegans* embryo by mutational analysis. *J. Cell Biol.* **144**, 927-946.

Gönczy, P., Bellanger, J. M., Kirkham, M., Pozniakowski, A., Baumer, K., Phillips, J. B. and Hyman, A. A. (2001). *zyg-8*, a gene required for spindle positioning in *C. elegans*, encodes a doublecortin-related kinase that promotes microtubule assembly. *Dev. Cell* **1**, 363-375.

Hamill, D. R., Severson, A. F., Carter, J. C. and Bowerman, B. (2002). Centrosome maturation and mitotic spindle assembly in *C. elegans* require SPD-5, a protein with multiple coiled-coil domains. *Dev. Cell* **3**, 673-684.

Hannak, E., Kirkham, M., Hyman, A. A. and Oegema, K. (2001). Aurora-A kinase is required for centrosome maturation in *Caenorhabditis elegans*. *J. Cell Biol.* **155**, 1109-1116.

Hsu, J. Y., Sun, Z. W., Li, X., Reuben, M., Tatchell, K., Bishop, D. K., Grushcow, J. M., Brame, C. J., Caldwell, J. A., Hunt, D. F. et al. (2000). Mitotic phosphorylation of histone H3 is governed by Ipl1/aurora kinase and Glc7/PP1 phosphatase in budding yeast and nematodes. *Cell* **102**, 279-291.

Kamath, R. S., Martinez-Campos, M., Zipperlen, P., Fraser, A. G. and Ahringer, J. (2001). Effectiveness of specific RNA-mediated interference through ingested double-stranded RNA in *Caenorhabditis elegans*. *Genome Biol.* **2**, RESEARCH0002.

Kawasaki, I., Shim, Y. H., Kirchner, J., Kaminker, J., Wood, W. B. and Strome, S. (1998). PGL-1, a predicted RNA-binding component of germ granules, is essential for fertility in *C. elegans*. *Cell* **94**, 635-645.

Kemp, C. A., Kopish, K. R., Zipperlen, P., Ahringer, J. and O'Connell, K. F. (2004). Centrosome maturation and duplication in *C. elegans* require the Coiled-Coil protein SPD-2. *Dev Cell* **6**, 511-523.

Kemphues, K. J., Wolf, N., Wood, W. B. and Hirsh, D. (1986). Two loci required for cytoplasmic organization in early embryos of *Caenorhabditis elegans*. *Dev. Biol.* **113**, 449-460.

Kile, B. T., Schulman, B. A., Alexander, W. S., Nicola, N. A., Martin, H. M. and Hilton, D. J. (2002). The SOCS box: a tale of destruction and degradation. *Trends Biochem. Sci.* **27**, 235-241.

Kirby, C., Kusch, M. and Kemphues, K. (1990). Mutations in the *par* genes of *Caenorhabditis elegans* affect cytoplasmic reorganization during the first cell cycle. *Dev. Biol.* **142**, 203-215.

Kitagawa, R., Law, E., Tang, L. and Rose, A. M. (2002). The Cdc20 homolog, FZY-1, and its interacting protein, IFY-1, are required for proper chromosome segregation in *Caenorhabditis elegans*. *Curr. Biol.* **12**, 2118-2123.

Kurz, T., Pintard, L., Willis, J. H., Hamill, D. R., Gönczy, P., Peter, M. and Bowerman, B. (2002). Cytoskeletal regulation by the Nedd8 ubiquitin-like protein modification pathway. *Science* **295**, 1294-1298.

Leidel, S. and Gönczy, P. (2003). SAS-4 is essential for centrosome duplication in *C. elegans* and is recruited to daughter centrioles once per cell cycle. *Dev. Cell* **4**, 431-439.

Lieberfarb, M. E., Chu, T., Wreden, C., Theurkauf, W., Gergen, J. P. and Strickland, S. (1996). Mutations that perturb poly(A)-dependent maternal mRNA activation block the initiation of development. *Development* **122**, 579-588.

Liu, J., Vasudevan, S. and Kipreos, E. T. (2004). CUL-2 and ZYG-11 promote meiotic anaphase II and the proper placement of the anterior-posterior axis in *C. elegans*. *Development* **131**, 3513-3525.

Lyczak, R., Gomes, J. E. and Bowerman, B. (2002). Heads or tails: cell polarity and axis formation in the early *Caenorhabditis elegans* embryo. *Dev. Cell* **3**, 157-166.

McCarter, J., Bartlett, B., Dang, T. and Schedl, T. (1999). On the control of oocyte meiotic maturation and ovulation in *Caenorhabditis elegans*. *Dev. Biol.* **205**, 111-128.

Nurse, P. (2002). Cyclin dependent kinases and cell cycle control. *Chembiochem* **3**, 596-603.

O'Connell, K. F., Maxwell, K. N. and White, J. G. (2000). The *spd-2* gene is required for polarization of the anteroposterior axis and formation of the sperm asters in the *Caenorhabditis elegans* zygote. *Dev. Biol.* **222**, 55-70.

Page, A. W. and Orr-Weaver, T. L. (1996). The *Drosophila* genes *grauzone* and *cortex* are necessary for proper female meiosis. *J. Cell Sci.* **109**, 1707-1715.

Pellettieri, J. and Seydoux, G. (2002). Anterior-posterior polarity in *C.*

elegans and *Drosophila* – PARallels and differences. *Science* **298**, 1946-1950.

Pellettieri, J., Reinke, V., Kim, S. K. and Seydoux, G. (2003). Coordinate activation of maternal protein degradation during the egg-to-embryo transition in *C. elegans*. *Dev. Cell* **5**, 451-462.

Peter, M., Castro, A., Lorca, T., Le Peuch, C., Magnaghi-Jaulin, L., Doree, M. and Labbe, J. C. (2001). The APC is dispensable for first meiotic anaphase in Xenopus oocytes. *Nat. Cell Biol.* **3**, 83-87.

Peters, J. M. (2002). The anaphase-promoting complex: proteolysis in mitosis and beyond. *Mol. Cell* **9**, 931-943.

Pichler, S., Gönczy, P., Schnabel, H., Pozniakowski, A., Ashford, A., Schnabel, R. and Hyman, A. A. (2000). OOC-3, a novel putative transmembrane protein required for establishment of cortical domains and spindle orientation in the P(1) blastomere of *C. elegans* embryos. *Development* **127**, 2063-2073.

Pintard, L., Kurz, T., Glaser, S., Willis, J. H., Peter, M. and Bowerman, B. (2003a). Neddylation and deneddylation of CUL-3 is required to target MEI-1/Katanin for degradation at the meiosis-to-mitosis transition in *C. elegans*. *Curr. Biol.* **13**, 911-921.

Pintard, L., Willis, J. H., Willems, A., Johnson, J. L., Srayko, M., Kurz, T., Glaser, S., Mains, P. E., Tyers, M., Bowerman, B. et al. (2003b). The BTB protein MEL-26 is a substrate-specific adaptor of the CUL-3 ubiquitin-ligase. *Nature* **425**, 311-316.

Praitis, V., Casey, E., Collar, D. and Austin, J. (2001). Creation of low-copy integrated transgenic lines in *Caenorhabditis elegans*. *Genetics* **157**, 1217-1226.

Rappleye, C. A., Tagawa, A., Lyczak, R., Bowerman, B. and Aroian, R. V. (2002). The anaphase-promoting complex and separin are required for embryonic anterior-posterior axis formation. *Dev. Cell* **2**, 195-206.

Rose, L. S. and Kemphues, K. J. (1998). Early patterning of the *C. elegans* embryo. *Annu. Rev. Genet.* **32**, 521-545.

Sadler, P. L. and Shakes, D. C. (2000). Anucleate *Caenorhabditis elegans* sperm can crawl, fertilize oocytes and direct anterior-posterior polarization of the 1-cell embryo. *Development* **127**, 355-366.

Schumacher, J. M., Ashcroft, N., Donovan, P. J. and Golden, A. (1998). A highly conserved centrosomal kinase, AIR-1, is required for accurate cell cycle progression and segregation of developmental factors in *Caenorhabditis elegans* embryos. *Development* **125**, 4391-4402.

Schwob, E., Bohm, T., Mendenhall, M. D. and Nasmyth, K. (1994). The B-type cyclin kinase inhibitor p40SIC1 controls the G1 to S transition in *S. cerevisiae*. *Cell* **79**, 233-244.

Shakes, D. C., Sadler, P. L., Schumacher, J. M., Abdolrasulnia, M. and Golden, A. (2003). Developmental defects observed in hypomorphic anaphase-promoting complex mutants are linked to cell cycle abnormalities. *Development* **130**, 1605-1620.

Shelton, C. A. and Bowerman, B. (1996). Time-dependent responses to glp-1-mediated inductions in early *C. elegans* embryos. *Development* **122**, 2043-2050.

Strome, S., Powers, J., Dunn, M., Reese, K., Malone, C. J., White, J., Seydoux, G. and Saxton, W. (2001). Spindle dynamics and the role of gamma-tubulin in early *Caenorhabditis elegans* embryos. *Mol. Biol. Cell* **12**, 1751-1764.

Taieb, F. E., Gross, S. D., Lewellyn, A. L. and Maller, J. L. (2001). Activation of the anaphase-promoting complex and degradation of cyclin B is not required for progression from Meiosis I to II in Xenopus oocytes. *Curr. Biol.* **11**, 508-513.

Timmons, L., Court, D. L. and Fire, A. (2001). Ingestion of bacterially expressed dsRNAs can produce specific and potent genetic interference in *Caenorhabditis elegans*. *Gene* **263**, 103-112.

Wallenfang, M. R. and Seydoux, G. (2000). Polarization of the anterior-posterior axis of *C. elegans* is a microtubule-directed process. *Nature* **408**, 89-92.

Wirbelauer, C., Sutterluty, H., Blondel, M., Gstaiger, M., Peter, M., Reymond, F. and Krek, W. (2000). The F-box protein Skp2 is a ubiquitylation target of a Cul1-based core ubiquitin ligase complex: evidence for a role of Cul1 in the suppression of Skp2 expression in quiescent fibroblasts. *EMBO J.* **19**, 5362-5375.

Wright, A. J. and Hunter, C. P. (2003). Mutations in a beta-tubulin disrupt spindle orientation and microtubule dynamics in the early *Caenorhabditis elegans* embryo. *Mol. Biol. Cell* **14**, 4512-4525.

Yang, H. Y., McNally, K. and McNally, F. J. (2003). MEI-1/katanin is required for translocation of the meiosis I spindle to the oocyte cortex in C elegans. *Dev. Biol.* **260**, 245-259.

Zhou, P. and Howley, P. M. (1998). Ubiquitination and degradation of the substrate recognition subunits of SCF ubiquitin-protein ligases. *Mol. Cell* **2**, 571-580.